Low dissolved Fe and the absence of diatom blooms in remote Pacific waters of the Southern Ocean

de Baar, Henricus; de Jong, Jeroen T.M.; Nolting, Rob F.; Timmermans, Klaas R.; van Leeuwe, Maria; Bathmann, U.; Rutgers van der Loeff, Michiel; Sildam, Jüri

Published in:
Marine Chemistry

DOI:
10.1016/S0304-4203(99)00022-5

ELSEVIER

Marine Chemistry 66 (1999) 1–34

MARINE CHEMISTRY

Low dissolved Fe and the absence of diatom blooms in remote Pacific waters of the Southern Ocean

Hein J.W. de Baar [a,b,*], Jeroen T.M. de Jong [a], Rob F. Nolting [a], Klaas R. Timmermans [a], Maria A. van Leeuwe [a,b], U. Bathmann [c], Michiel Rutgers van der Loeff [c], Jüri Sildam [c,1]

[a] *Netherlands Institute for Sea Research (NIOZ), PO Box 59, 1790 AB Den Burg (Texel), Netherlands*
[b] *Department of Marine Biology, University of Groningen, Groningen, Netherlands*
[c] *Alfred Wegener Institute for Polar and Marine Research, Bremerhaven, Germany*

Received 22 October 1997; received in revised form 24 February 1999; accepted 2 March 1999

Abstract

The remote waters of the Pacific region of the Southern Ocean are the furthest away from any upstream and upwind continental Fe sources. This prime area for expecting Fe limitation of the plankton ecosystem was studied (March–April 1995) along a north–south transect at ~89°W. At the end of the austral summer the upper wind-mixed layers were in the order of ~100 m deep, thus mixing the algae down into the dimly lit part of the euphotic zone where photosynthesis is severely restricted. The dissolved Fe was found at low concentrations ranging from 0.05 nM near the surface to 0.5 nM in deeper waters. Along the transect (52°S–69°S), the dissolved iron was enhanced in the Polar Front, as well as near the Antarctic continental margin (0.6–1.0 nM). In between, the southern ACC branch was depleted with iron; here the concentrations in surface waters were quite uniform at about 0.21 nM. This is only somewhat lower than the 0.49 nM (October 1992) and 0.31 nM (November 1992) averages in early spring in the southern ACC part of Atlantic 6°W sections [de Baar, H.J.W., de Jong, J.T.M., Bakker, D.C.E.. Löscher, B.M., Veth, C., Bathmann, U., Smetacek, V., 1995. Importance of iron for phytoplankton spring blooms and CO_2 drawdown in the Southern Ocean. Nature 373, 412–415; Löscher, B.M., de Jong, J.T.M., de Baar, H.J.W., Veth, C., Dehairs, F., 1997. The distribution of iron in the Antarctic Circumpolar Current. Deep-Sea Research II 44, 143–188.]. First, the lower ~0.21 nM in March–April 1995 may partly be due to continuation of the seasonal trend where the phytoplankton growth, albeit modest, was removing Fe from the surface waters. Secondly, the 89°W Pacific stations are further downstream continental or seafloor sources than the Atlantic 6°W section. In the latter case, the ACC water had passed through the Drake Passage and also over the Sandwich Plateau. Indeed for Drake Passage, intermediate Fe concentrations have been reported by others. The generally somewhat lower surface water Fe at the ACC and PF at 89°W is consistent with the distance from sources and the late summer. It also would explain the very low abundance of phytoplankton (Chl *a*) in the region and the conspicuous absence of plankton blooms. In the subAntarctic waters north of the Polar Front there are no diatoms, let alone diatom blooms, due to low availability of silicate. Thus, it

* Corresponding author. Netherlands Institute for Sea Research (NIOZ), PO Box 59, 1790 AB Den Burg (Texel), The Netherlands. Tel.: +31-222-369465; Fax: +31-222-319674; E-mail: debaar@nioz.nl
[1] Current address: Dalhousie University, Halifax, Nova Scotia, B3H 4J1 Canada.

PII: S0304-4203(99)00022-5

appears the biological productivity is suppressed due to iron deficiency, in combination with the severe seasonal effects of wind mixing on the light climate, as well as regional silicate limitation for diatoms.

Keywords: diatom; dissolved Fe; Southern Ocean

1. Introduction

1.1. Distribution of Fe in the biosphere

The abundance of iron (Fe) in the upper biosphere is closely linked with the evolution of oxygen. In the primordial ocean, there was no free oxygen present and high concentrations of reduced dissolved Fe(II) in seawater were readily available for incorporation in biota during the first stages of biological evolution (Löscher et al., 1997). This has led to Fe having several key functions in all biota as known nowadays. For example, the similar high availability of dissolved sulfide S(II) in the ancient oceans, now appears consistent with the ubiquity of the Fe–S-rich ferredoxin in all biological systems (Wächtershäuser, 1992; Russell et al., 1993; Edwards, 1998). However, largely due to photosynthesis, more and more free oxygen (O_2) was becoming available removing Fe from solution as solid Fe(III) oxyhydroxide phases. In the modern well-oxygenated ocean, the Fe is very unstable in solution as it tends to precipitate out into solid Fe(III) phases (Millero et al., 1995). Consequently, in modern open ocean waters, the very low abundance of nanomolar dissolved Fe, largely due to oxygenation by plant evolution, may have become limiting for plant life itself. On the other hand, photochemical reduction may still lead to substantial concentrations of Fe(II) in oceanic surface waters (Waite et al., 1995). On land with a crustal abundance of Fe averaging at $\sim 5.6\%$ (Taylor, 1964), this partly consisting of Fe-oxide coating on minerals, the land biota remain to have an ample supply of Fe, notably because many groundwaters are anoxic such that dissolved Fe(II) is readily available for uptake by plant roots. Moreover, in anaerobic marine sediments or semi-enclosed basins high concentrations of dissolved Fe(II) are known to persist. Such anoxic sediments as well as some anoxic semi-enclosed basins like the Black Sea (Lewis and Landing, 1991) may be seen as the lower biosphere which is still as oxygen-free as the primordial planet. Thus due to the anoxic nature of marine sediments at continental margins, quite some dissolved Fe may diffuse out and reach the upper euphotic zone of the water column, thus providing adequate Fe for phytoplankton growth in coastal waters. Therefore, when traversing from land and rivers into coastal waters, over the continental shelf and slope into the open ocean, one expects the dissolved concentration of Fe to become less and less. Continents being the major source of Fe it is expected that in the most remote oceans, notably the remote Pacific sector of the Southern Ocean, the concentration of Fe in surface waters is the lowest and most limiting for plant life.

1.2. Limitation by Fe in the remote Southern Ocean

The hypothesis of iron limitation of Antarctic ecosystems (Gran, 1931; Martin and Fitzwater, 1988; de Baar, 1994) was first tested in 1988/1989 in the Weddell Sea, the Scotia Sea and the intermediate front or Weddell–Scotia Confluence (de Baar et al., 1989, 1990; Buma et al., 1991). In all five experimental runs, iron supply stimulated phytoplankton growth. Close examination of the data from Fe enrichments over the first few days showed only minor iron-mediated increases in algal stocks, as also observed elsewhere (Martin and Fitzwater, 1988). In all incubations eventually a shift towards larger size classes of essentially diatoms was observed and ascribed to exclusion of mesozooplankton grazers, the shift being most pronounced in the iron enriched bottles, suggesting a superimposed stimulation by iron of larger diatoms (Buma et al., 1991). From the latter observations, the daily rate of cell division of the dominant diatoms was calculated to be about 10% enhanced in the Fe enriched bottles, suggesting suboptimal growth rates in the field situation. This

direct effect of Fe on the largest size class of bloom-forming diatoms would be consistent with the concept of diffusion limitation (Harvey, 1937), being most severe for larger cells with low specific surface area (Hudson and Morel, 1990). The Fe stimulation was most prominent in the more offshore Confluence and Scotia Sea, where ambient dissolved iron were low albeit still neritic at >1 nM (Nolting et al., 1991) as compared to higher iron levels in more nearshore waters of the Weddell Sea (Westerlund and Öhman, 1991; Nolting et al., 1991) similar to inshore Gerlache Strait at the Pacific side of the Peninsula (Martin et al., 1990a). In this frontal region, both dissolved Fe (Nolting et al., 1991) and particulate Al levels were found to be quite high (Dehairs et al., 1992). At 49°W at the Scotia Front, then at $\sim$ 49°S, a subsurface maximum of particulate Al as high as 30 nM was found at $\sim$ 200 m depth (Dehairs et al., 1992, their Fig. 8) and ascribed to upstream shelf sediment sources of the Peninsula and Archipelago region. Assuming 10% dissolution and the given Fe:Al ratio, there is the potential to bring between 1.1 and 4.2 nM Fe into solution (Dehairs et al., 1992). This is comparable to the dissolved Fe measured in the region (Nolting et al., 1991).

In the more offshore waters of Drake Passage, in the austral summers of 1990 and 1991, Helbling et al. (1991) found significant effects of either 1 or 5 nM Fe additions at their sites C and D, but no or little effect of iron addition at their inshore sites A, F or nearshore sites B, E ($\sim$ 1000 m water depth). This is consistent with, respectively, the lower dissolved Fe $\sim$ 0.1–0.88 nM in offshore Drake Passage waters and higher dissolved iron at $\sim$ 4.7–7.4 nM in inshore Gerlache Strait (Martin et al., 1990a). At their offshore site C, the Fe enrichment selectively stimulated the larger microplankton, as opposed to the control incubation. Hence, from this experiment alone, it would appear that in the field the microplankton are limited predominantly by iron stress, rather than selectively removed by mesozooplankton grazing. This would tentatively characterize the offshore Drake Passage as oligotrophic for iron.

In the austral summer of 1990, a suite of four incubation experiments was done in the Ross Sea (Martin et al., 1990b). The results were similar to the previous observations in the Weddell/Scotia Seas. Iron always stimulated plankton growth, most strongly at the more offshore station (St. 98 in Ross Sea), but the untreated controls also showed a steady increase of biomass exceeding in situ chlorophyll *a* levels. Dugdale and Wilkerson (1990) correctly interpreted the findings in terms of grazing pressure, and the changes thereof in the incubations, such that iron stress would appear to be less dominant in the field situation. Unfortunately, there is no information on ambient levels of dissolved iron. Particulate iron levels (Martin et al., 1991) are higher ($\sim$ 0.7–2.7 nM) inshore than at the offshore site (<0.5 nM) suggesting a decrease in dissolved iron with distance offshore, consistent with the more pronounced effect of Fe enrichment at the offshore site.

In the austral spring of 1992, the first Southern Ocean JGOFS expeditions took place (Bathmann et al., 1994; Turner et al., 1995; Smetacek et al., 1997). For the Atlantic sector an integrated study of the plankton ecosystem along a truly offshore, large scale, section (>1000 km length at $\sim$ 6°W) was designed. Here the spatial distribution of ambient dissolved iron in the upper 300 m of the water column was consistent with the oceanographic position of the Polar Front, local diatom blooms and significant CO_2 undersaturations vs. the atmosphere (de Baar et al., 1995). These observations in an unperturbed system constituted the first ever evidence that Fe supply stimulates plankton blooms and causes uptake of CO_2 from the atmosphere (Bakker et al., 1997). The underlying causal relationships were demonstrated in a suite of shipboard mesocosm incubations with excellent reproducibility underlining the effectiveness of clean procedures (van Leeuwe et al., 1997; Scharek et al., 1997). The Polar Frontal jet at about 49–50°S, meandering eastward across the 6°W section, was characterized by elevated dissolved iron of $\sim$ 1.87 nM in Section 5/6 and decreasing to $\sim$ 1.14 nM two to three weeks later (Löscher et al., 1997). This decrease was consistent with a general increase of particulate plankton matter measured as POC and PON or Chl *a* (Bathmann et al., 1997) and occurrence of major blooms of large diatoms *Corethron criophilum* (Crawford et al., 1997) and *Fragilariopsis kerguelensis* (Bathmann et al., 1997; de Baar et al., 1997a). Over the spring period, a general decrease of major nutrients, and anomalous removal ratios of nitrate and phosphate (de Baar et al., 1997a) were observed exactly at the

Polar Front. Simultaneously, the distributions of particulate and dissolved ^{234}Th had shown pronounced scavenging of ^{234}Th on the biogenic particles (Rutgers van der Loeff et al., 1997). This supports the contention of similar removal of dissolved iron, by uptake into or adsorption onto planktonic particles. This was partly confirmed by the large percentage of easily leachable particulate iron on suspended particles, compared to the more southerly oligotrophic ACC waters (Löscher et al., 1997). Otherwise, the total particulate Fe was significantly higher at the Polar Front, as was the total particulate Al determined in the same samples (Löscher et al., 1997). This particulate Al was independently confirmed in samples collected with different samplers and analyzed separately by F. Dehairs at the same stations (Löscher et al., 1997). The strong signal of particulate Al suggested a continental source term for latter Al, as well as for the particulate Fe and the dissolved Fe. Similarly, the higher concentrations of lithogenic silica were also found here (Quéguiner et al., 1997). From the oceanographic consistency of all these chemical and biological features with the hydrography of the Polar Frontal jet and eddies (Veth et al., 1997), a source term of Fe within the oceans is suggested. Recent contact of these waters with conti-

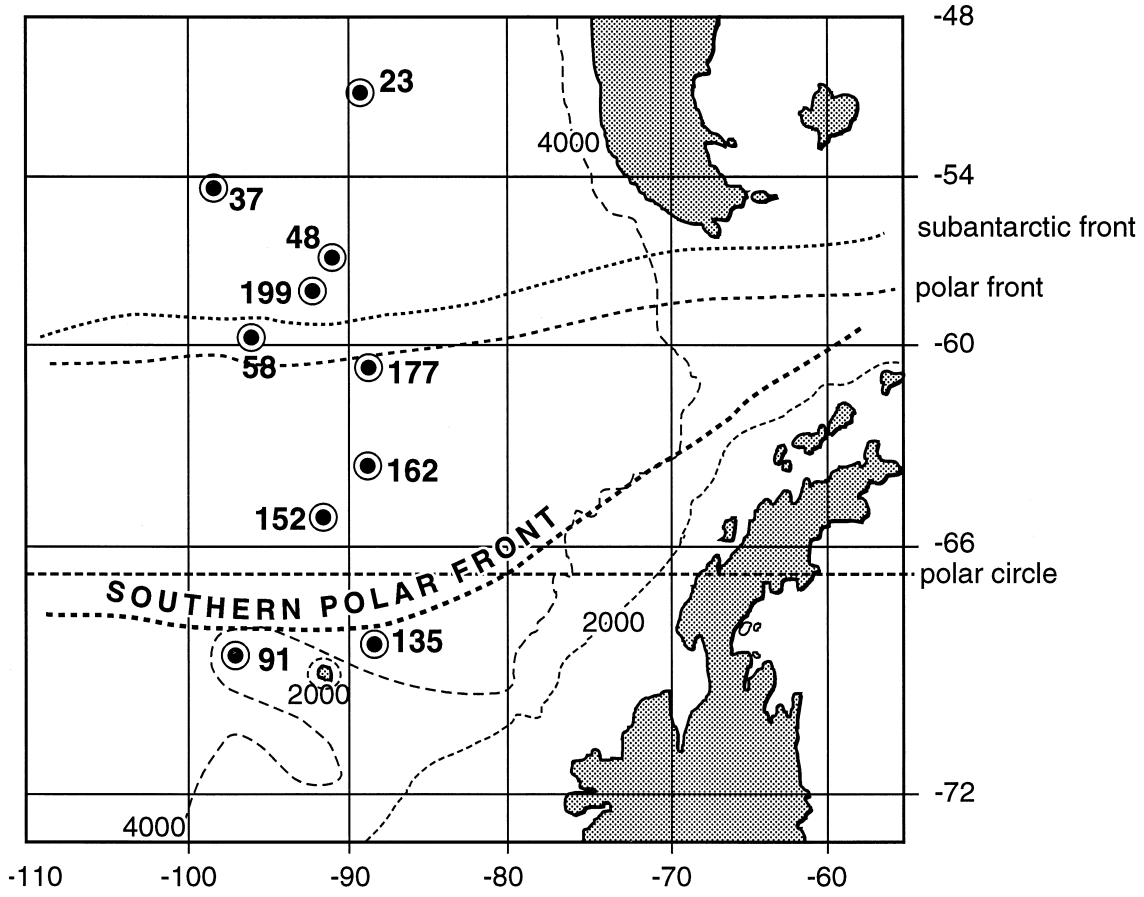

Fig. 1. Chart of the research area with sites of the 10 stations. Also shown are the approximate positions of the major fronts: the subantarctic Front (SAF) separating the subantarctic Zone (SAZ) from the Polar Frontal Zone (PFZ), the Polar Front separating the PFZ from the southern Antarctic Circumpolar Current (sACC) and the southern Polar Front (sPF). The latter virtually coincides with the Continental Water Boundary (CWB) separating the sACC from the Bellingshausen Sea. Due to the limited number of occupied stations the locations of the fronts during the period of the cruise are known only by approximation. For this reason the CWB is not shown at all but expected to be at about 70°S, just south of the sACC Front and at or near the sites 91 and 135.

nental margin sediments of the Argentine basin is conceivable (de Baar et al., 1995). However, an aeolian source of Fe originating from the South American continent cannot be excluded either (Duce and Tindale, 1991; Kumar et al., 1995; Löscher et al., 1997). In contrast, in the southern branch of the ACC (~ 51–56°S) the dissolved Fe levels were much lower, decreasing seasonally from an average of 0.49 nM to an average of 0.31 nM some weeks later (de Baar et al., 1995). The lowest observed dissolved Fe was 0.17 nM. The mean surface water levels at ~ 0.31 or ~ 0.49 nM were adequate to sustain a low and constant phytoplankton biomass (Chl $a < 0.25$ $\mu g\ l^{-1}$), but were insufficient for bloom development (de Baar et al., 1995). Summarizing the previous Antarctic studies it appears that waters near, or frontal systems downstream the Antarctic Peninsula or the South-American shelf exhibit elevated Fe concentrations. This is in contrast to the southern ACC in the Atlantic Antarctic sector, or the middle of Drake Passage, which both are regions further away from upstream or upwind Fe sources.

1.3. The 1995 JGOFS Southern Ocean study

The very remote waters of the Pacific region of the Southern Ocean are the furthest away from any conceivable upstream and upwind continental Fe sources. Therefore, an expedition aboard RV Polarstern was set up in order to investigate this prime area for expecting Fe limitation of the Antarctic plankton ecosystem. At the end of the austral summer season (March–April 1995) a north–south transect at ~ 89°W was investigated, crossing the Subantarctic Front and Polar Front areas, the Antarctic Circumpolar Current (ACC) and closer to the continent, entering into the Bellingshausen Sea (Fig. 1). In this project, the reported distributions of dissolved Fe were combined with an assessment of the organic complexation of Fe (Nolting et al., 1998), short-term bioassays (incubations) of the indigenous plankton community using physiological indicators (Timmermans et al. (1998), taxonomic determination of phytoplankton groups using photopigments (van Leeuwe et al., 1998a), as well as determination of the possible effect of Fe limitation on chromatic adaptation by the natural plankton communities (van Leeuwe et al., 1998b). Aspects of this work were presented previously at the American Chemical Society and the Gordon Research Conference for Chemical Oceanography (Timmermans et al., 1997; de Baar et al., 1997b). The significance of the work within the global context of Fe–biota studies and CO_2 cycling has been addressed by van Leeuwe (1997) and de Baar and Boyd (1999).

2. Materials and methods

2.1. Preparations

Prior to the cruise the PVC samplers (GoFlo 12 L, General Oceanics) had been modified and cleaned. The samplers were coated with teflon from a spray container, and the drain cock was replaced by an all-Teflon stop cock (Chemfluor). The external black rubber string was deemed to be a source of contamination and found to loose its strength by increasing age and the cold ambient seawater temperatures, and therefore replaced by a titanium spring. For mounting on the 10-mm thick Kevlar hydrowire special PVC blocks with stainless steel bolts were attached to the samplers. Kevlar wire is more sensitive to abrasion than steel wire, for which reason a 10 mm thickness is preferred. The samplers had been cleaned inside the home clean air laboratory by filling with 0.01 M HCl, soaking for at least 24 h and rinsing with deionised (Milli-Q) water. At the first test-station, all GoFlo samplers were filled with seawater and subsequently acidified to pH 2 with HCl and left to stand for another 24 h. Before use, they were drained and rinsed extensively with Milli-Q water.

All labware and bottles to be in contact with the seawater had been precleaned in the home laboratory by immersion at 60°C for at least 24 h into either 7 N HNO_3 (Teflonware) or 6 N HCl (polyethylene, PE). Then the labware was brought into the clean air laboratory, rinsed with Milli-Q water and allowed to dry to the air in a Class-100 laminar flow bench. The bottles were packaged individually into a PE bag and then stored in a plastic box. Then, the boxes with labware and bottles were brought into the laboratory van which was transported to the research vessel. The Milli-Q system of the shipboard laboratory van is connected to a storage tank (60 l) as to allow recycling of the Milli-Q water several times before use.

The necessary reagents had been purified in the laboratory. The 12 N HCl and 14 N HNO_3 stocks were distilled threefold in an all-quartz subboiling distillation apparatus and collected into Teflon FEP storage bottles. The Fe concentration in these 3QD stocks was determined for each batch by evaporation to dryness of a subsample of 30 ml in a Teflon vial, re-dissolution in 1 ml 1 N 3 QD HNO_3 and detection by Graphite Furnace Atomic Absorption Spectrometry. These blanks were ~ 3 nM and ~ 25 nM for HNO_3 and HCl, respectively. Preparation of all other reagents is described below.

2.2. Sampling

Seawater samples were collected at 10 stations in the upper 800 m of the water column (Table 1). Immediately upon arrival at the station, the trace metal sampling was the first activity undertaken. The samplers were attached at standard distance to the Kevlar hydrowire (10 mm) lowered from a special winch with a 35-kg lead-filled PVC counterweight at the end of the wire. The nominal depths were 25, 50, 75, 150, 200, 300, 400, 600 and 800 m. The string was kept in place for 5–10 min, where some vertical and lateral movement along with the drifting surface vessel may allow any inadvertent contamination from shipboard handling to get rinsed off by the ambient seawater. Before tripping, the wire angle was verified as to avoid large offsets between nominal and true depths. The samplers were tripped with large size Teflon messengers containing a titanium ballast core. The deepest sampler was equipped with a SIS pressure sensor, tripping at the same time as the closing of the bottle, in order to verify the proper depth of sampling.

At the same stations and four other sites, an additional CTD/Rosette hydrocasts down to 600 m was taken for determination of salinity and temperature (averaged at 2-m intervals) and derived values of potential temperature and density, as well as analyses of nutrients at 12 depths. These observations in combination with the underway thermosalinograph registration of the surface waters were used to characterize the general hydrography.

Upon recovery, the GoFlo samplers were detached from the hydrowire and immediately returned to their fixed positions in closable storage cabinets on the outside of the class 100 clean air container van. The air vent stoppers at the top of the samplers were replaced by screwing in a connector piece attached to precleaned silicone tubing for the N_2 gasline system to be used during filtration. Teflon tubing was connected to the lower stopcocks in order to drain the seawater into the laboratory van. Inside this van special lab coats, clogs and plastic gloves were used. The Teflon tubing had been stored in a tank with dilute HCl and was rinsed with Milli Q water before first use. Between stations the outside ends of the Teflon tubing were connected in pairs with silicone tubing as to allow soaking and flushing from the inside laboratory. When sampling, a volume of about 500 ml of the seawater was passed through the tubing to allow extensive rinsing. Part of this rinse water was collected for the nutrient analyses. Next, the unfiltered seawater was used to rinse a precleaned polyethylene sampling bottle threefold before filling up for analysis of total dissolvable (unfiltered) Fe.

2.3. Filtration

Subsequently, the teflon tubing was connected to a filter cartridge holder containing a precleaned polycarbonate membrane filter with 0.2 μm or 0.4 μm pore size. The parts of the filter cartridges had been stored in a tank with dilute HCl and were always rinsed with Milli Q water before use. Upon discarding the first filtrate effluent, the precleaned polyethylene bottle was rinsed threefold and filled. During filtration the GoFlo's were pressurized with < 0.5 bar overpressure by N_2 gas from cylinders of highest purity grade led over an in-line particle arrestance filter cartridge.

The sample bottles were placed inside a laminar flow bench and acidified to pH 1.8 with the 3QD 14 N HNO_3 (1 ml l^{-1}) using an Eppendorf pipette with acid-cleaned tip. The calculated contribution to the seawater value was ~ 3 pM which is negligible compared to the lowest detected concentration of 0.05 nM (50 pM).

2.4. Analysis

Within 1 h after sampling and filtration, the Fe concentrations were determined by flow injection

analysis (FIA) with in-line preconcentration and chemiluminescence (CL) detection, after Obata et al. (1993). The instrument (Fig. 2) is an assembly of standard components and was placed next to a laminar flow bench in which the reagents were prepared and samples were handled. An 8-channel peristaltic pump drives reagents, sample and rinsing water via a combination of 4-port and 6-port valves towards the reaction coil and then the detector. The reagents were maintained at constant 30°C temperature inside a thermostat-controlled acrylic cabinet. Acidified seawater mixes with dilute ammonium acetate buffer to raise the pH to 4.2 before passing a 7 cm long, 3 mm i.d. preconcentration column of 8-hydroxyquinoline immobilised on hydrophylic vinyl polymer (TSK-8-HQ) after Landing et al. (1986). After 4 min loading, about 15 ml sample had been extracted. Then the valve was switched and the column first rinsed with Milli Q water for 1 min to remove sea salts before elution with dilute 0.2 N HCl in reverse flow direction. The eluate is mixed with ammonia, hydrogen peroxide and a luminol/triethylene–tetramine (TETA) mixture, then flowing via the reaction coil in a 30°C water bath into the CL flow cell mounted inside a Hamamatsu C695B photomultiplier refrigerator containing a Hamamatsu R268P photomultiplier tube kept at -20°C.

2.5. Reagents

The 0.2 N HCl was prepared from the 3QD 12 N HCl stocks. The 0.4 N NH_4OH by dilution of 25% Suprapure (Merck) and 0.7% H_2O_2 by diluting 30% stock (Baker Analyzed). TETA (Merck) was used as purchased. Concentrated ammonium acetate buffer stock was prepared by passing high purity ammonium gas via a filter cartridge into 3QD acetic acid in a teflon FEP bottle placed inside a ~ 0°C ice/water bath. After about 1 h, the solution had become highly viscous and the gas flow was shut off. From this, a 25-fold dilution was prepared using Milli-Q water. The luminol was purified by dissolution of 15 g in 500 ml Milli-Q in a 2000 ml teflon bottle with the addition of 2 g K_2CO_3 (pro analysis). The luminol was recrystallized by addition of 15 ml 3QD HCl, carefully as to avoid the mixture to overflow the bottle. The solution was stirred gently for 1 h, then filtered over an acid-cleaned GF/F filter and rinsed with Milli-Q water. This procedure was repeated once, then the luminol was allowed to dry to the air within a clean air bench, ground in an acid-cleaned Teflon mortar and stored in a PE bottle. Working solution was prepared from ~ 130 mg luminol and ~ 200 mg K_2CO_3 in a small volume of Milli Q, then further diluted to 1 l in a Nalgene PP volumetric flask and allowed to stand for 24 h for removing any remaining Fe by adsorption to the wall of the vessel (Powell et al., 1995). The solution was further purified by passing over a Chelex-100 column and finally the 100 μl TETA was added. This purification of the luminol, albeit laborious, led to a tenfold decrease of the baseline signal of the FIA-CL.

2.6. Performance

The optimised conditions reported by Obata et al. (1993) were verified with a batch of filtered Sargasso Sea water (Fe = 0.57 nM). The selectivity of the TSK-8HQ column was confirmed by scanning the CL response over a pH range of 1.3 to 8 (Fig. 3). Here, two plateaus were found at $2.6 < pH < 4.5$ where only Fe(III) is quantitatively extracted, and at $6 < pH < 7$ where both Fe(II) and Fe(III) are being extracted (Obata et al., 1993). Matrix interference was verified for metals Cr, Mn, Co, Ni, Cu and not detectable at pH 3.2 and 6.3 but significant at pH 8 representative of natural seawater. Therefore, all samples were first acidified to pH 1.8 and analyzed at pH 3.5–4.0 as to ensure that all dissolved Fe was extracted in the Fe(III) state and then detected. The immobilized 8-hydroxyquinoline has very high affinity to Fe and the resulting values are deemed to represent the complete dissolved fraction, although less than 100% extraction efficiency, due to competing very strong natural organic ligands, cannot be ruled out.

The unfiltered samples had been kept at pH 1.8 for at least 1 h in which most of the particulate Fe would have dissolved, except possibly a minor refractory mineral component. Therefore, the unfiltered values are referred to as total dissolvable Fe. Because the particulate Fe in seawater is thought to be a continuum in the size spectrum from larger mineral particles to plankton cells to colloids, the here reported dissolved Fe is operationally defined as < 0.4 μm. Nevertheless, the abundance of biogenic

Table 1
The 10 stations where Fe was determined with dates of sampling, bottom depth, latitude, longitude, nominal sampling depths and concentrations as follows

Station (number) (date) depth [m]	Latitude °S	Longitude °W	Depth (m)	Fe < 0.4 (nM)	Fe total (nM)	SiO_4 (μM)	NO_3 (μM)	PO_4 (μM)
23; 27.3.95; 4829	51°55′	89°24′	−25			1.60	17.10	1.18
			−50					
			−75			2.80	18.00	1.24
			−100	0.55		5.40	19.60	1.37
			−150			6.40	21.40	1.41
			−200	0.28		7.00	21.70	1.44
			−300			7.50	22.10	1.46
			−400	0.19		7.70	22.30	1.53
			−600	0.32		11.40	25.30	1.66
			−800			20.60	29.60	1.94
37; 29.3.95; 4704	54°20′	89°39′	−25					
			−50	0.31		2.20	17.30	1.28
			−75					
			−100	0.30		5.90	17.30	1.28
			−150	0.16		6.90	22.00	1.54
			−200	0.27		7.00	22.00	1.53
			−300			7.40	22.40	1.54
			−400	0.20		7.60	22.60	1.55
			−600					
			−800	0.20		21.70	30.00	2.05
48; 1.4.95; 4918	57°16′ S	91°14′ W	−25			3.70	21.00	1.49
			−50	0.29		4.20	21.20	1.50
			−75	0.11		4.60	21.90	1.55
			−100	0.10		5.70	23.30	1.63
			−150	0.13		6.10	24.60	1.73
			−200	0.21		12.20	26.90	1.86
			−300	0.31		16.40	28.60	1.96
			−400	0.25		22.50	30.50	1.07
			−600	0.20		33.60	33.20	2.26
			−800	0.23		47.50	35.40	2.45
199; 6.5.95; 4786	57°58′	91°51′	−25	0.11	0.14	4.80	22.60	1.56
			−50	0.10	0.62	4.70	22.80	1.57
			−75	0.10	0.39	4.80	22.70	1.57
			−100	0.07	0.38	4.90	22.60	1.58
			−150		0.28	5.10	22.60	1.58
			−200	0.23	0.48	8.90	25.20	1.73
			−250	0.21	0.47	13.10	27.20	1.84
			−300	0.17	0.55	15.80	28.60	1.92
			−400	0.40	0.68	20.80	29.50	2.00
			−600	0.30	0.57	37.80	33.40	2.27
			−800	0.47	0.72	52.90	35.30	2.41
58; 6.4.95; 4733	59°44′	96°03′	−25			4.00	20.80	1.47
			−50	0.34		3.90	20.80	1.47
			−75	0.30		3.90	20.90	1.46
			−100					
			−150	0.16		3.90	21.10	1.49
			−200			10.10	25.30	1.71
			−300	0.35		14.50	27.30	1.86
			−400	0.28		20.00	28.90	1.96
			−600					
			−800	0.32		46.90	34.40	2.34

Table 1 (continued)

Station (number) (date) depth [m]	Latitude °S	Longitude °W	Depth (m)	Fe < 0.4 (nM)	Fe total (nM)	SiO_4 (μM)	NO_3 (μM)	PO_4 (μM)
177; 29.4.95; 5013	60°58′	89°29′	−25	0.05		10.70	26.00	1.81
			−50	0.06		10.70	26.00	1.85
			−75	0.13		10.70	26.20	1.87
			−100	0.08		10.80	26.10	1.89
			−150	0.13		20.30	29.10	2.06
			−200	0.13		22.50	29.80	2.09
			−300	0.07	0.46	24.10	30.20	2.10
			−400	0.18	0.39	30.40	31.50	2.21
			−600	0.23	0.37	46.60	35.50	2.45
			−800	0.26	0.27	62.00	36.30	2.57
162; 25.4.95; 4957	63°59′	89°31′	−25	0.15	0.29	11.80	26.80	1.89
			−50	0.16	0.57	11.90	26.30	1.90
			−75	0.16	0.32	11.70	26.60	1.91
			−100	0.24	0.45	11.50	26.50	1.90
			−150	0.37	0.50	19.90	29.30	2.06
			−200	0.39	0.41	23.50	35.00	2.12
			−300	0.27	0.50	27.00	31.70	2.17
			−400	0.2	0.52	45.60	35.00	2.46
			−600	0.28	0.53	62.50	36.60	2.60
			−800	0.33	2.05	70.90	37.00	2.58
152; 21.4.95; 4765	65°24′	91°10′	−25	0.19		13.00	25.50	1.80
			−50	0.17		12.70	25.10	1.80
			−75	0.18		12.80	25.30	1.80
			−100	0.16		22.60	29.00	2.05
			−150	0.17		26.80	36.00	2.13
			−200	0.3		35.90	32.10	2.28
			−300	0.2		57.20	36.40	2.53
			−400	0.18		65.60	37.20	2.59
			−600	0.25		75.40	35.60	2.55
			−800	0.21		80.70	35.60	2.49
135; 18.4.95; 4716	68°16′	89°24′	−50	0.21		33.00	26.10	1.90
			−75	0.25		54.00	32.80	2.25
			−100	0.41		59.50	34.30	2.36
			−150	0.31		67.60	36.70	2.50
			−200	0.86		75.10	37.10	2.54
			−300	0.29		81.20	36.50	2.51
			−400	0.43		83.90	35.90	2.46
			−600	0.39		87.60	34.70	2.38
			−800	0.47		91.80	34.50	2.35
91; 9.4.95; 3871	68°31′	97°10′	−25	0.22		18.70	23.60	1.63
			−50	0.12		19.40	24.00	1.67
			−75	0.15		27.30	26.00	1.89
			−100					
			−150	0.11		53.20	33.50	2.32
			−200	0.51		66.50	36.40	2.52
			−300	0.15		76.40	36.40	2.52
			−400	0.42		79.30	36.30	2.45
			−600	0.19		85.00	34.30	2.38
			−800	0.31		87.80	33.40	2.33

Dissolved Fe (nM) in the fraction filtered over 0.4 μ nominal pore size membrane filters, total dissolvable Fe (nM) in unfiltered seawater, silicate (μM), nitrate (μM) and phosphate (μM).

We report all measured data without rejecting any due to perceived ‘too high’ values. Rather where occasional higher values are encountered there is no justification for their rejection, and it is more rewarding to assess these values within oceanographic context.

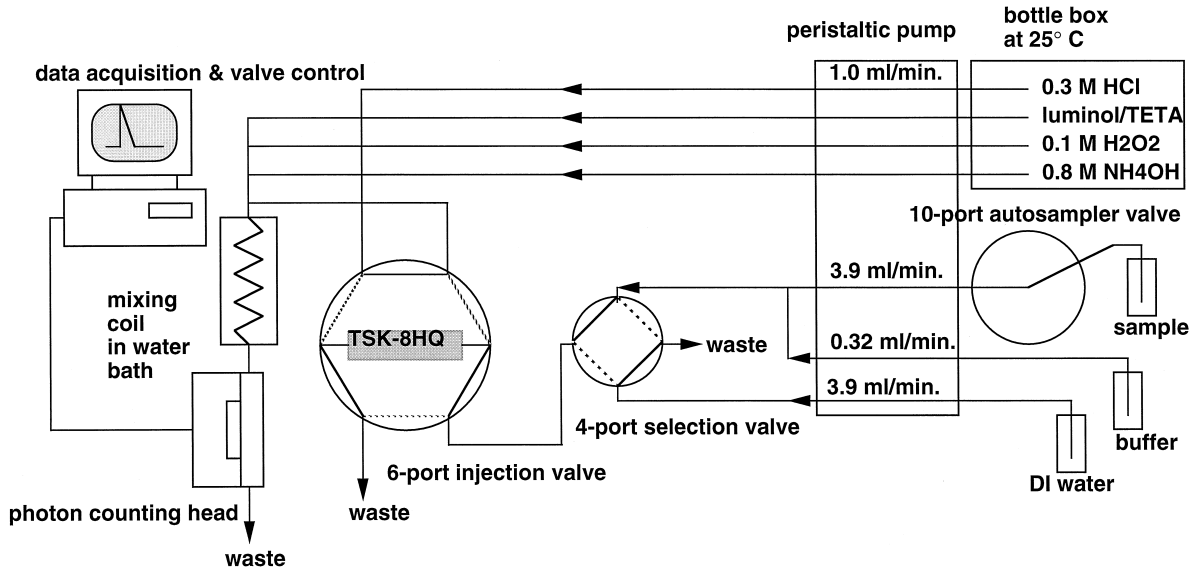

Fig. 2. Configuration of the FIA-CL analysis.

and mineral particles is extremely low in these most remote Antarctic waters and the nominal 0.4 μm cutoff would be more realistic than in any other oceanic region.

The analytical blank was determined 55 times during the expedition with a mean value of 0.05 nM and a standard deviation of 0.005 nM. The detection limit defined as threefold latter standard deviation was 0.015 nM. The 0.05 nM blank was caused by the Milli-Q water used for rinsing the column before elution and was confirmed by detecting the peak height that resulted from loading the column for 1 min with MilliQ water. The blanks of the 14 N QD HNO_3 and the dilute ammonium acetate buffer were found negligible by comparing the signal from a normally processed sample with the same sample treated with extra acid and buffer, respectively. This was furthermore consistent with the reagent blanks determined in the home laboratory by evaporating the acid and buffer to dryness and analyzing the Fe contents by GFAAS. The stability of the background signal and blank allowed reproducible analysis of even the lowest reported 0.05 nM concentration. For consecutive analyses of the same sample, the reproducibility was within 5% standard deviation over the whole 0.05–2 nM working range.

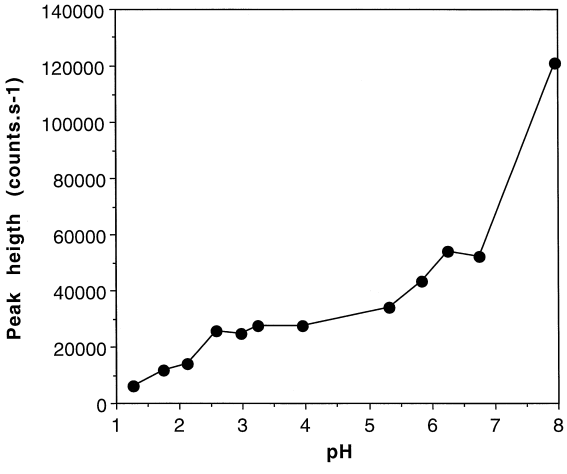

Fig. 3. The sensitivity of the signal of the FIA-CL to pH for a Sargasso seawater sample containing Fe at 0.57 nM.

Calibration standard solutions were prepared from a stock solution of 1000 mg l^{-1} Fe(III) (J.T. Baker Dilut-It) into a standard of 179.1 μM in 0.1 N HCl. From this a working standard of 200 nM was prepared in 0.1 N HCl. From this standard additions were made to filtered and acidified low-Fe seawater in precleaned PP volumetric flasks to addition values of 0.25–0.5–1.0–2.0 nM. Accuracy was validated using reference seawater NASS-4 certified at 1.88 ± 0.29 nM. During this expedition we found 1.81 ±

0.15 nM ($n = 4$). Also six samples previously collected, filtered and analyzed by APDC/DDDC with GFAAS (Löscher et al., 1997, their station 905 at 48°S 6°W) were redetermined two years later with FIA-CL. These samples were not meant to be redetermined and had been stored during the two years in half-empty bottles such that evaporation may have occurred, also some refractory minerals may slowly have further dissolved. Nevertheless a convincing agreement was found (Fig. 4). In both cruises, identical sampling and filtration were used, the current findings (Table 1, Fig. 4) further confirming the overall reproducibility of both datasets. However, the analytical blank and detection limit of the FIA-CL method are lower than published blanks for the APDC/DDDC-GFAAS method of 0.08 ± 0.02 nM ($n = 9$) and 0.28 ± 0.005 nM ($n = 8$) reported by pioneers Martin and Gordon (1988) and typically 0.12 ± 0.04 nM ($n = 6$) recently reported by Löscher et al. (1997). In a more recent cruise (Polarstern ANT XIII/2, January 1996; Weddell Sea and Polar Front), the same FIA-CL method had a lower blank of 0.022 nM ($n = 10$) with a somewhat higher standard deviation of 0.07 nM and detection limit of 0.022 nM due to the lower number (10 instead of 55) of blank determinations (de Jong et al., 1998).

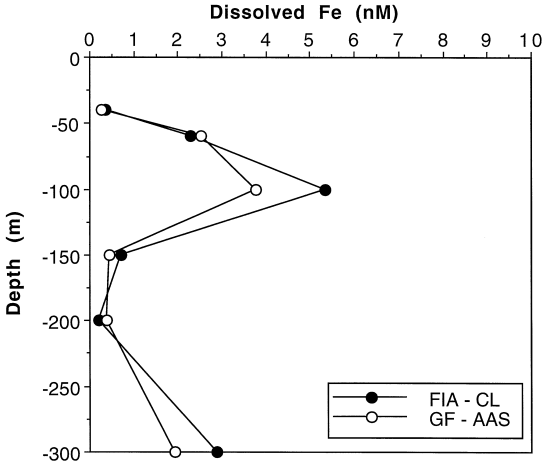

Fig. 4. Redetermination by FIA-CL (filled dots) of six samples previously collected, filtered and analyzed by APDC/DDDC with GFAAS (Löscher et al., 1997) and since then stored half-full without the objective of an actual redetermination. Station 905 at 48°S, 6°W sampled at 29 October 1992 during Polarstern ANT X/6. The sampling and filtration procedures of ANT X/6 and ANT XII/4 (this work) were identical, only the final determination method is different. The generally good agreement confirms the overall quality of both datasets (Löscher et al., 1997, and this work).

2.7. Hydrography, nutrients, ^{234}Thorium, chlorophyll a and phytoplankton species

Salinity (conductivity), temperature and depth (pressure) were determined in separate hydrocasts at 40 stations (Table 2) with a SeaBird 911 CTD mounted in a 12 bottles Rosette sampler (Sildam, 1995). The pressure-protected thermistor sensor and a Paroscientific Digiquartz pressure and conductivity sensor had been calibrated by Seabird before and after the cruise. Specified accuracies were 0.0003 S/m for conductivity, 0.002°C for temperature and 0.015% for pressure at full scale (here 6800 dbar). At the deep CTD stations, the values were checked vs. reversing thermometers and salinity from bottle values determined with a Guildline Autosal 8400 Salinometer. While passing a transect, the salinity and temperature of the surface water were recorded with an automated thermosalinograph coupled to a computer for data storage.

Samples for nutrients were determined within 12 h after collection by J. van Ooyen (NIOZ) with a TRAACS 800 automated analyzer and methods after Grashoff et al. (1983). The reproducibility was 0.20 μM for nitrate, 0.10 μM for ammonia, 0.05 μM for phosphate and 0.3 μM for silicate. The nutrient values of the GoFlo casts and the CTD/Rosette casts showed good agreement for the given 10 stations, confirming the approximate sampling depths of the GoFlo samplers as well as their proper closing.

The radioactivity of dissolved and particulate ^{234}Th (dpm l^{-1}) were determined by Rutgers van der Loeff and associates with a MnO_2-coprecipitation technique described elsewhere (Rutgers van der Loeff et al., 1997; Rutgers van der Loeff and Moore, in press). Briefly, 15–25 l samples were filtered over a 142 mm diameter 1 μm poresize nuclepore membrane. To a weighed aliquot of the filtrate (approx. 20 l) were added 6 drops of concentrated ammonia (25 wt.% of NH_3) and 250 μl of concentrated $KMnO_4$ solution (60 g/l), followed after mixing by 100 μl concentrated $MnCl_2$ solution (400 g $MnCl_2$ ·

Table 2
Listing of positions of 30 stations for ancillary data of hydrography, among which 24 stations where Chl *a* and Phaeophytin data are available here, listed only as depth-integrated inventories

Station	Latitude	Longitude	Chl *a* (mg/m^2)	Phaeophytin (mg/m^2)
14	50°09′S	89°12′W	11.15	6.37
17	50°39′S	89°16′W	13.22	5.08
19	51°09′S	89°18′W		
21	51°25′S	89°21′W	12.31	6.69
23	51°54′S	89°24′W		
26	52°25′S	89°27′W	13.33	8.18
28	52°53′S	89°30′W	11.08	6.82
30	53°24′S	89°34′W	11.47	4.56
32	53°49′S	89°35′W	9.40	10.65
37	54°19′S	89°39′W	11.73	10.16
45	55°28′S	89°46′W	13.44	8.82
47	55°39′S	89°49′W		
55	57°53′S	93°30′W	13.90	8.54
60	61°30′S	97°41′W	13.96	6.13
80	66°31′S	97°26′W	11.10	5.26
91	68°31′S	97°10′W	11.10	5.26
103	69°24′S	95°01′W		
104	69°25′S	94°10′W	16.88	9.35
135	68°16′S	89°23′W	8.08	5.07
138	67°59′S	92°39′W	12.82	5.73
141	67°13′S	91°50′W	13.56	7.35
154	65°09′S	90°43′W	9.95	3.87
162	63°59′S	89°32′W	14.88	4.13
166	63°02′S	89°34′W		
172	62°03′S	89°30′W	17.25	5.38
177	61°01′S	89°30′W	18.38	3.85
182	60°16′S	89°31′W	13.83	5.17
186	59°27′S	89°32′W	12.99	6.43
207	57°27′S	89°16′W		
210	57°03′S	88°01′W	23.53	9.03

Among these 30 stations there are 10 the same as in Table 1 for the actual Fe data.

$5H_2O$/l). The resulting MnO_2 precipitate was allowed to grow for 8 h and filtered over a second 142-mm nuclepore filter. Both filters, containing the suspended particles and the MnO_2 precipitate, respectively, are dried, folded and beta counted on board. The value of ^{238}U activity (dpm l^{-1}) of its radioactive parent was calculated from salinity using the relationship $A_U = 0.0704 \times S$ after Chen et al. (1986).

The chlorophyll *a* and phaeophytin was measured by M. Templin and U. Bathmann (Alfred Wegener Institute) according to Holm-Hansen et al. (1965). The phytoplankton species composition has been assessed in the parallel study by van Leeuwe et al. (1998a), relying on a combination of flow cytometry, microscopic counts, and HPLC photopigment characterization.

3. Results

3.1. Hydrography

All waters south of the Subtropical Front (at ~40°S) constitute the Southern Ocean. The water masses, fronts and circulation of the ~90°W region of the Southern Ocean have been well described by Read et al. (1995). An overview of all circumpolar waters and fronts has been given by Orsi et al.

(1995). The ~40°S to 70°S latitude range is dominated by the Antarctic Circumpolar Current (ACC) and its fronts, flanked into equatorial direction by the Subtropical Front and towards Antarctica by the Continental Water Boundary (CWB). The eastward flowing ACC extends throughout the complete water column and four major frontal systems of the ACC are also perceptible at all depths. These are the SubAntarctic Front (SAF), the Polar Front (PF), the Southern Polar Front (sPF) and the Continental Water Boundary (CWB) (Fig. 1). To the north of the SAF lies the corresponding interfrontal zone, the SubAntarctic Zone. To the north of the PF lies the northern branch of the ACC, or the Polar Frontal Zone (PFZ). South of the PF lies the southern branch of the ACC (sACC) or the Antarctic Zone which at its most southern extent exhibits the sPF quite close to the true boundary of the ACC, the CWB. The Continental Zone south of the CWB is not part of the ACC.

The Polar Front is the northern boundary of the Antarctic Ocean proper which at ~90°W thus constitutes the Antarctic Zone and the Continental Zone, the latter more or less comprising the geographic region of the Bellingshausen Sea extending eastward to the Antarctic Peninsula. The SubAntarctic Front (SAF) and Polar Front are well recognized circumpolar features, the CWB is a more regional front, for example in most of the Atlantic sector the ACC-Weddell Boundary (AWB) takes its function as southerly bound of the ACC (Veth et al., 1997).

Observations of Read et al. (1995) clearly indicate that at ~90°W, the Polar Front does consist of two branches, the northern branch (PF) and the southerly branch now referred to as Southern Polar Front (sPF) as already defined by Orsi et al. (1995) not only at this longitude but also as a circumpolar feature. On occasion, four distinct fronts had also been observed in Drake Passage, and the sPF was also found near the Greenwich meridian (Veth et al., 1997).

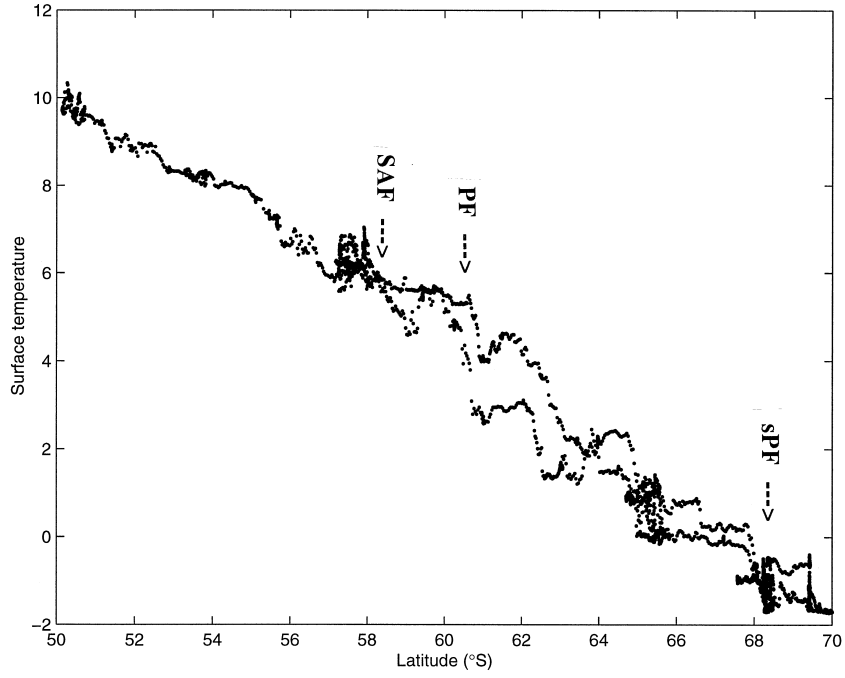

Fig. 5. Section plot of surface water temperature over the 50–70°S interval at the 90°W meridian. Compilation of several cruise tracks during period of ANT XII/4 expedition, with offsets due to autumn cooling most apparent in the 58–68°S region. Approximate position of fronts indicated by arrows: SAF (~58–59°S), PF (60°30′–61°S), sPF (~68°S), not shown is the CWB (~69°30′S). For each individual cruise track the exact position of each front could only be approximated due to limited resolution of CTD stations (see also Fig. 6). Between cruise tracks the true position of a front would also shift somewhat due to meandering (Veth et al., 1997).

At 90°W and elsewhere, all fronts exhibit temporal variability of their exact latitudinal position, also due to meandering. Nevertheless, the north–south transects of the surface water salinity and temperature of the thermosalinograph (Fig. 5) clearly showed distinct gradients at sites of fronts, which were closely resembling those of Read et al. (1995, their Fig. 7). However, their observations as well as most previous data (Eltanin sections, Gordon, 1967) were collected in the October–November season, while our data is from the March–May period. Therefore, the absolute values of salinity and temperature in surface waters are somewhat different due to seasonal warming/cooling and formation/melting of sea-ice. This difference was most noticeable at higher latitudes. The vertical distributions of salinity and potential temperature (Fig. 6) show surface water freshening at ~ 68–70°S with stabilization of the upper water column by the strong salinity gradient. At the other, subAntarctic part of the section (50° to ~58°S) there is a thermocline at much greater depth.

Following Read et al. (1995) and Orsi et al. (1995) and by comparison with their findings of the thermosalinograph, of vertical profiles of S, θ and density at 20 stations (Table 2), as well as of θ–S properties (not shown), the positions of the fronts were identified. The SAF was found to be situated at about 58°S to 59°S. This implies that station 199 (57°58′S, 91°51′W) and more northerly stations 23 (51°55′S, 89°24′W), 37 (54°20′S, 89°39′W) and 48 (57°16′S, 91°14′W) are within the SubAntarctic Zone. The depth of the wind-mixed layer was about 60 m at station 23 and 100 m at stations 37 and 48 (Fig. 7).

The surface water salinity 34.1 at site 199 fits the uniform same values of the thermosalinograph until

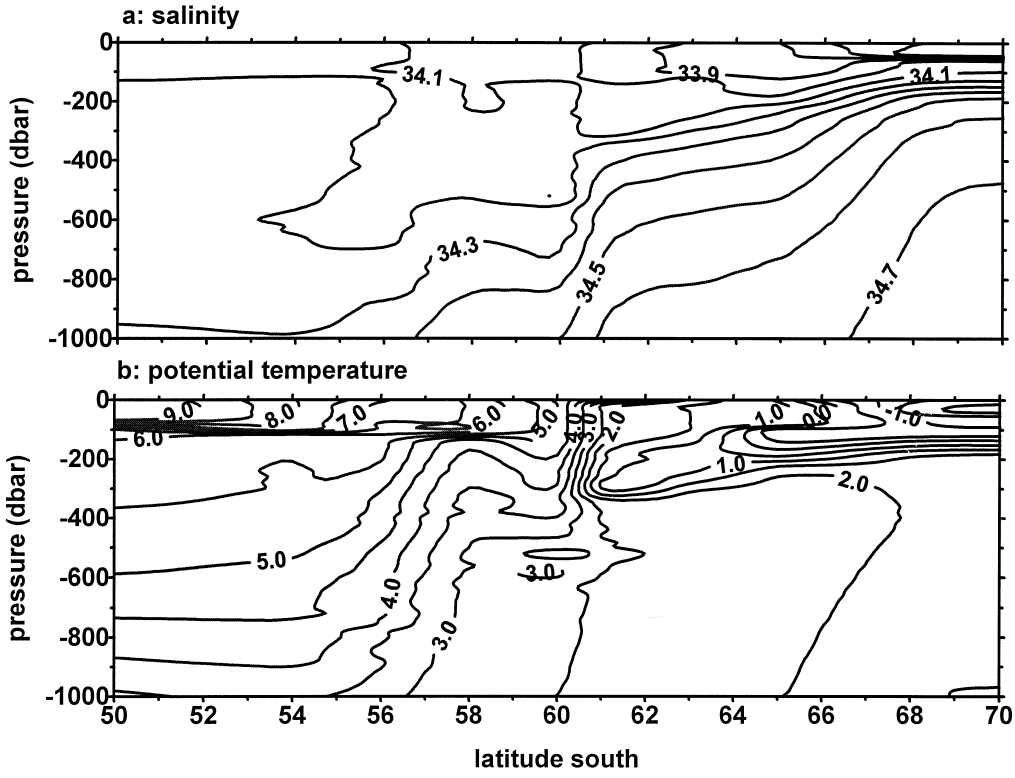

Fig. 6. Section plots of (a) salinity (upper) and (b) potential temperature (lower) in the upper 1000 metres over the 50–70°S interval at the 90°W meridian, on the basis of individual stations situated at or nearby 90°W (see Fig. 1). Note stratification of upper water column towards 69–70°S which is favorable for the light climate for phytoplankton growth. Approximate positions of fronts are: SAF (~58–59°S), PF (60°30′–61°S), sPF (~68°S), CWB (~69°30′S).

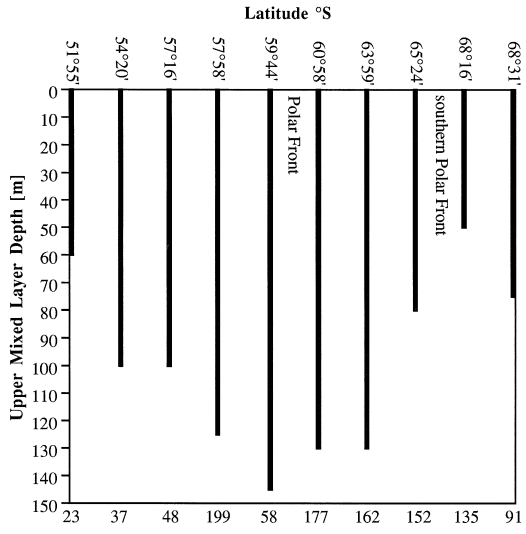

Fig. 7. The depth (m) of the Upper Wind Mixed Layer at the 10 stations along the transect where also the dissolved Fe was determined. Wind is a major forcing but various hydrographic factors (salinity and temperature gradients, density field, frontal systems) also strongly influence the observed depth of the upper mixed layer. Top horizontal axis is latitude (°S) simply ranked increasing towards the right, the corresponding station numbers are given at bottom horizontal axis, see also Table 1.

about 51°S within the SAZ, but is lower than the uniform ~34.2 value in the different austral spring season found in the SAZ by Read et al. (1995). The temperature of ~6.5°C at station 199 more closely resembles values during austral spring in the 57–59°S region of the SAZ (Read et al. (1995). Due to a three day hurricane before its sampling the station 199 (57°58′S) had an upper mixed layer extending to over 125 m depth (Fig. 7). Below the sharp thermocline in this depth range the temperature gradually decreases from 4°C at ~200 m to 3°C at ~800 m depth, consistent with trends at previous stations 37 and 48. At latter stations and more equatorward sites (Table 2) there is a weak salinity minimum at about 700–800 m indicative of the Antarctic Intermediate Water. At greater depths the salinity increases and this is consistent with a tongue of Pacific Deep Water (PDW) contributing to the Circumpolar Deep Water (CDW).

The PF was situated at about 60°30′ to 61°S, which implies that Station 58 (59°44′S, 96°03′W) is still within the Polar Frontal Zone and station 177 (60°58′S, 89°29′W) is at most just at, but more likely just south of, the Polar Front. At station 58, the wind-mixed layer extended even deeper down to 140–150 m. The stations 177 (60°58′S, 89°29′W) and much more southerly 162 (63°59′S, 89°31′W) exhibit almost identical vertical profiles of salinity and temperature and therefore both are taken as definitely within the Antarctic Zone, also called the southern ACC branch. Below a wind mixed layer of about 130 m at both stations (Fig. 7), the temperature decreases to a distinct minimum of 1°C at 300 m (177) and 250 m (162) depth. This is taken as the winter water of the Antarctic Zone (Whitworth, 1988) which more southerly is more distinct, at shallower depths (~100 m) with also lower temperatures (Fig. 6; see also Read et al., 1995, their Fig. 6). Going south within the sACC the surface temperature decreased steadily to about 1°C at stations 152 (65°24′S, 91°10′W)/154 (65°08′S, 90°41′W). Here, the thermosalinograph confirmed a strong drop of surface temperature with latitude which however is not being defined as a front (e.g., Read et al., 1995). At sites 152/154, the wind mixed layer was somewhat shallower down to about 80 m depth (Fig. 7). The winter water is at ~100 m depth with a very distinct minimum temperature of less than −1°C.

Near the 90°W meridian, the sPF and the CWB are known to be very close together and not easily resolved unless with high-resolution sampling at closely spaced stations (Orsi et al., 1995; see also their Fig. 11). During our cruise the Southern Polar Front was found to be at about 68°S, judging from lateral surface temperature gradients of the thermosalinograph (Fig. 5). The station 135 (68°16′S, 89°24′W) is situated more or less at the sPF. The surface minimum of −1.8°C is due to intense sea-ice formation and virtually complete sea-ice coverage at the time of sampling, and hardly any wind so that vertical mixing was nil. These conditions obscured the assignment of the exact location of the sPF. At station 91 (68°31′S, 97°10′W) the hydrographic conditions were very similar (except for the very surface waters) with the winter-water temperature minimum also at ~100 m depth, and both sites 135 and 91 are still within the southernmost part of the sACC. At station 135, there is very strong stratification (strong gradients of θ, S and density) in the surface layer, favorable for phytoplankton growth. On the other

hand at site 91 there is a wind-mixed layer down to about 75 m depth (Fig. 7).

At the surface, a strong temperature decrease was found at about 69°30′S. This and expected local

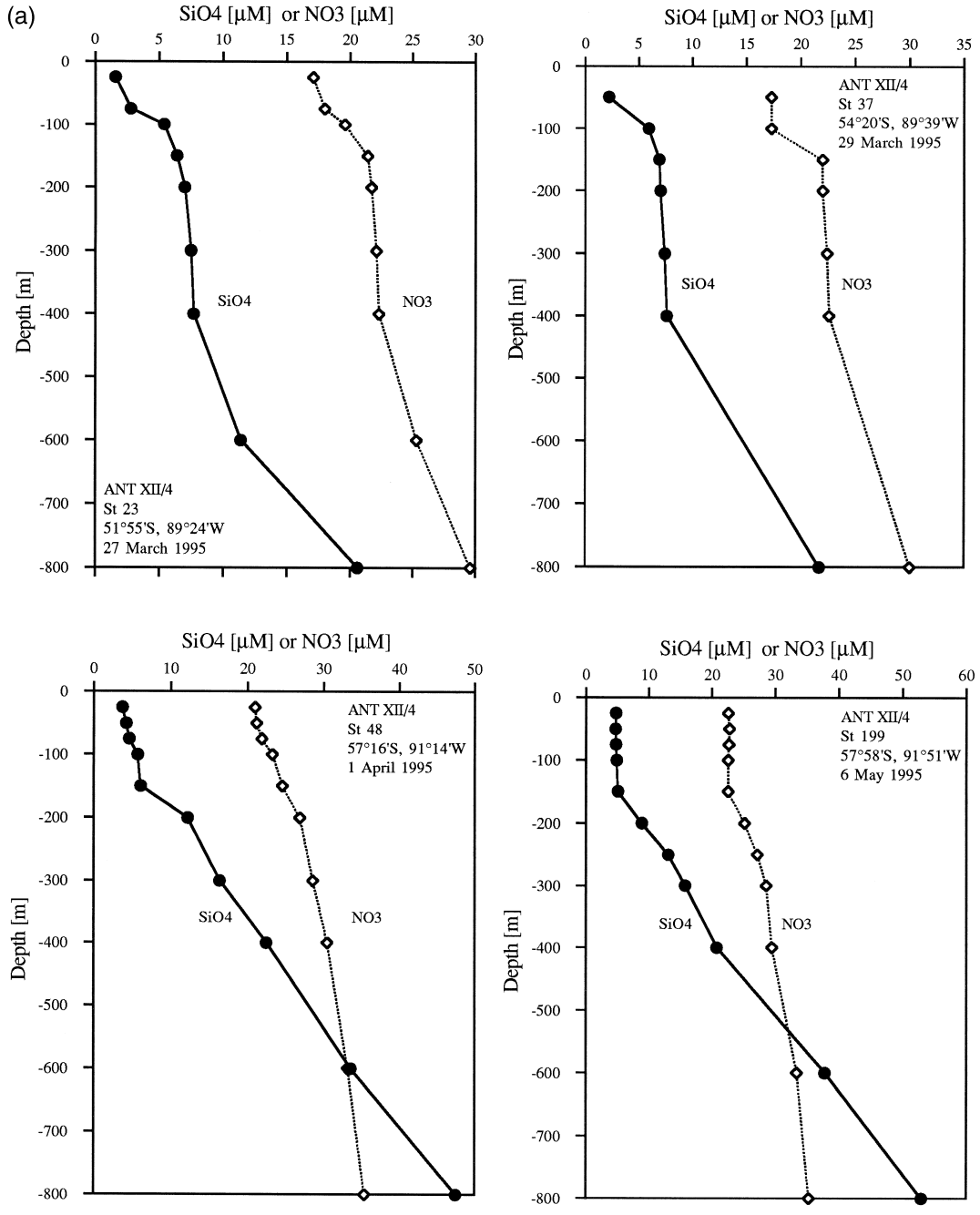

Fig. 8. Vertical distributions of nitrate (µM) and silicate (µM) at the 10 research stations where dissolved Fe had also been determined, for values see Table 1.

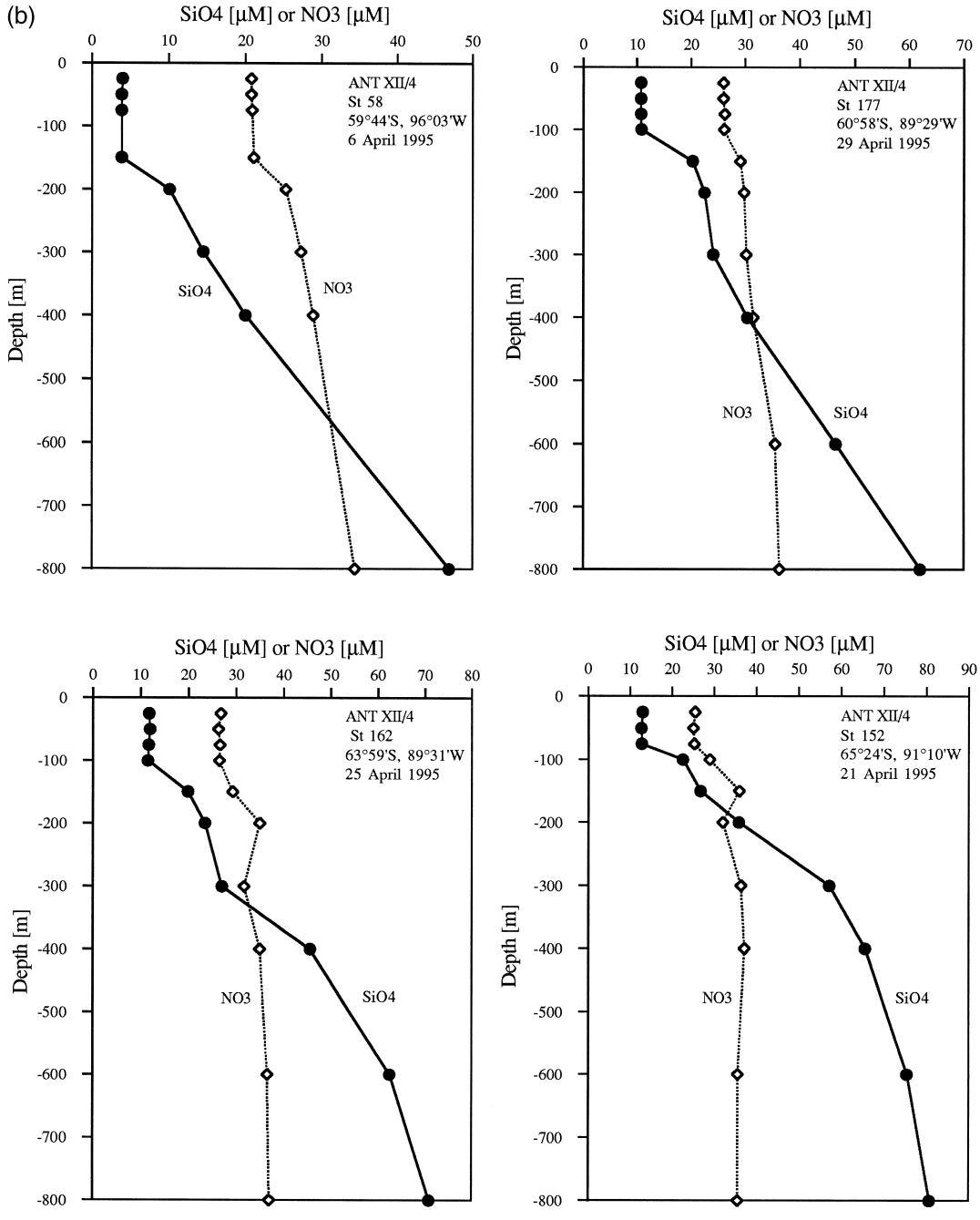

Fig. 8 (continued).

salinity gradients would mark the Continental Water Boundary but its exact location was obscured by ongoing processes of sea-ice formation. Also, the transect did not extend further south than 69°25′S at 94°10′W (station 104) and the CWB would not be discernible as a transition in a longer section. At

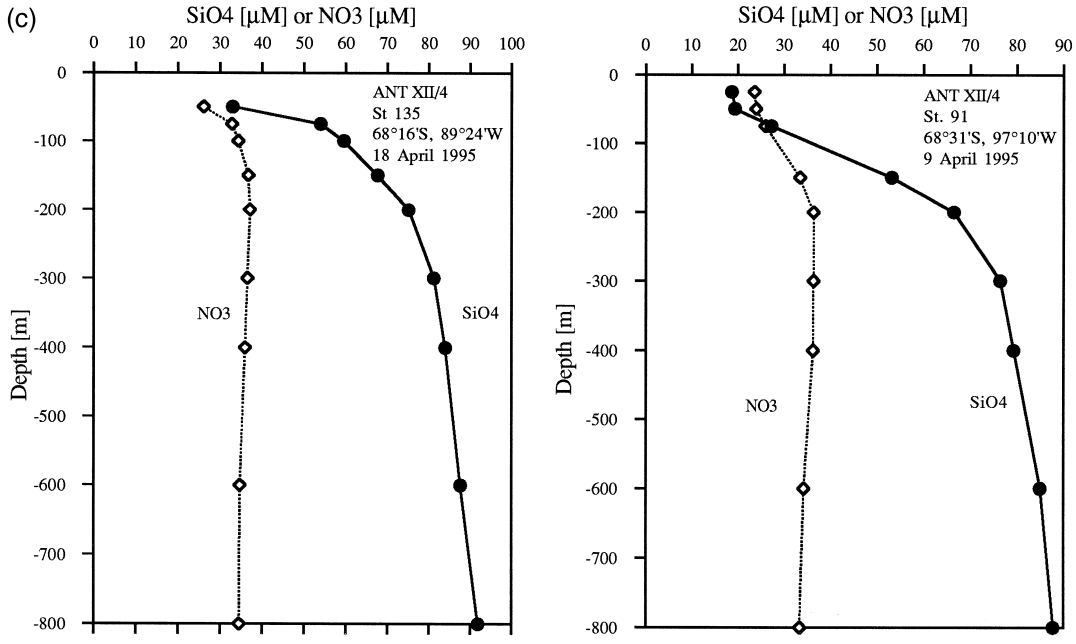

Fig. 8 (continued).

southernmost stations 103 and 104, the temperature minimum of the winter water at ~100 m depth is hardly (103) or no longer (104) a distinct minimum, presumably due to ongoing autumn cooling of the upper 100 m of the water column.

3.2. Major nutrients

Also for the nutrients, the circumpolar trends are well known. Within the Antarctic Ocean proper, south of the Polar Front, major nutrients are present all year; typical concentrations in surface waters are in the order of 1.6 to 2.0 µM phosphate, 20 to 30 µM nitrate and 30 to 100 µM silicate (Gordon et al., 1986; Kamykowski and Zentara, 1989; Levitus et al., 1993). In summer significant depletions due to biological uptake have been observed. In the Polar Frontal Zone the values decrease towards the Sub-Antarctic Front due to mixing with nutrient-poor waters of the north (Bathmann et al., 1994, their Fig. 6.5.5.; de Baar et al., 1997a, their Fig. 3). This gradient is most pronounced for silicate, most notably in the east Pacific region of our study (Plate 3 of Comiso et al., 1993; Sullivan et al., 1993, their Fig. 4B). Therefore, in the PFZ, silicate may well become limiting for diatom growth. In the adjacent Subantarctic Zone all major nutrients become more or less depleted. Hence, within the overall Southern Ocean, only the Antarctic Ocean proper, south of the Polar Front, is truly a region where HNLC conditions prevail for all major nutrients (de Baar and Boyd, 1999).

The distributions of nutrients at our stations are consistent with hydrography and above general expectations (Figs. 8 and 9). In surface water at station 37 (54°20′S, 89°39′W) the silicate is low at 2.2 µM which likely is limiting for growth of larger diatoms

Fig. 9. Section plots of the distributions of (a) silicate (µM), (b) nitrate (µM), (c) phosphate (µM) and (d) dissolved Fe (nM) in the upper 800 m of the water column. The isolines were drafted at intervals of 5 µM (silicate), 2.5 µM (nitrate), 0.1 µM (phosphate) and 0.05 nM (dissolved Fe). For dissolved Fe at 68°S the maxima at ~0.6–0.8 nM at 200 m depth (see also Fig. 14) cause the strong local gradient of fitted isolines. Approximate positions of fronts are: SAF (~58–59°S), PF (60°30′–61°S), sPF (~68°S), CWB (~69°30′S).

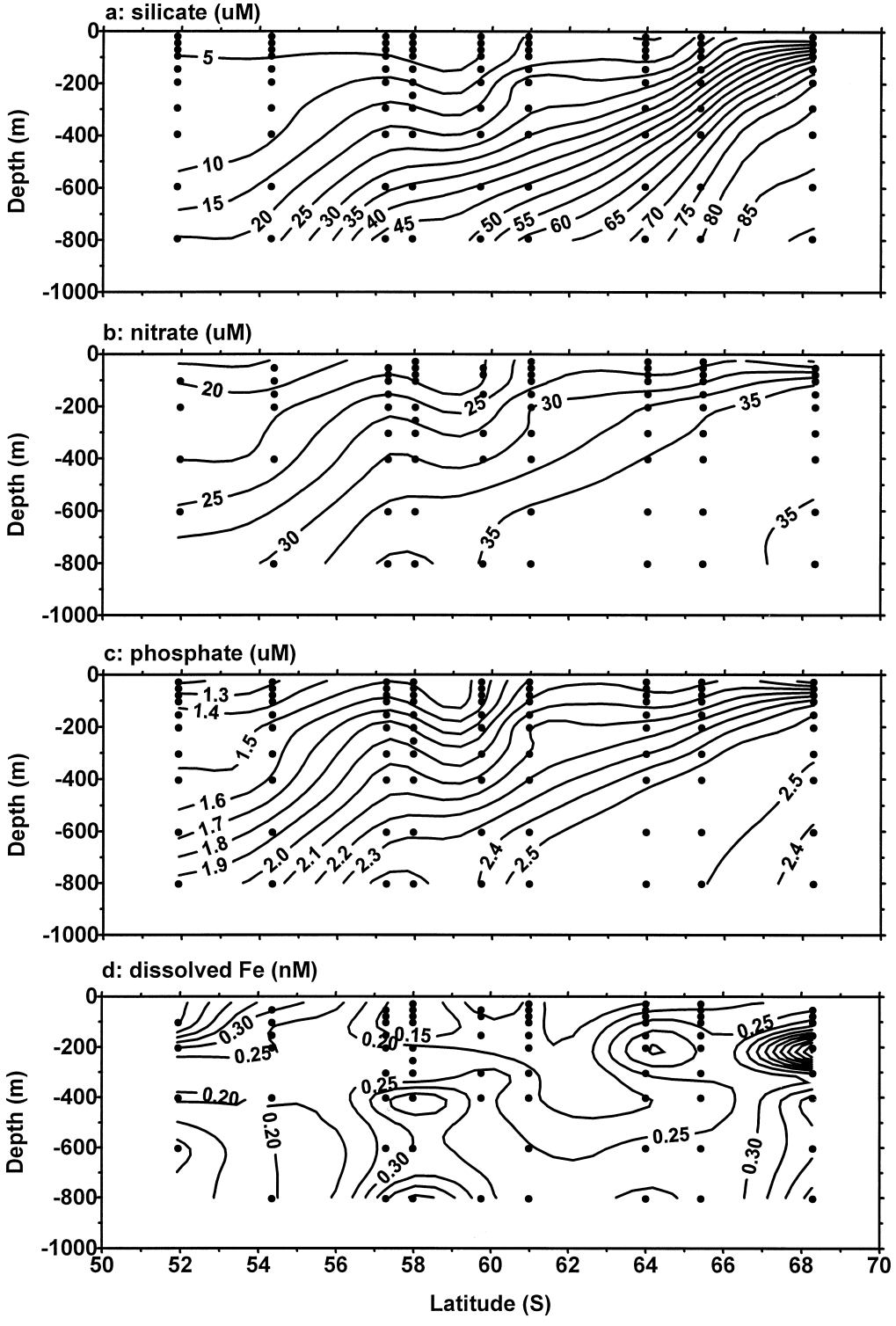
a: silicate (uM)
b: nitrate (uM)
c: phosphate (uM)
d: dissolved Fe (nM)
Depth (m)
Latitude (S)
0
-200
-400
-600
-800
-1000
50
52
54
56
58
60
62
64
66
68
70

(Nelson and Treguer, 1992; Brzezinski and Nelson, 1996). Even at 400 m depth, the silicate is no more than 7.4 μM. The nitrate and phosphate are more abundant at ~17.3 μM and 1.18 μM, respectively, and deemed to be not limiting at all for plant growth. At station 48 (57°16′S, 91°14′W), values of silicate are still quite low at ~4 μM in surface waters and may be suboptimal for diatoms, the nitrate and phosphate have become higher, suggesting more southern component water. At station 58 (59°44′S, 96°03′W), the silicate is still around 4 μM in surface waters. Finally, at station 177 (60°58′S, 89°29′W), just within the Antarctic Zone, the silicate exceeds 10 μM and would likely be in adequate supply also for the largest diatoms. At station 177, the surface values of nitrate and phosphate have also strongly increased compared to station 58. The surface waters of 177 (60°58′S, 89°29′W) and more southerly 162 (63°59′S, 89°31′W) have similar levels of major nutrients, but at both sites, the deep water values are higher. Likely, the cumulative biological removal during the preceding spring and summer accounts for this vertical gradient of major nutrients. This is even more apparent at stations 152, 135 and 91 in the southern ACC, most notably for silicate in the upper 100 m of the water column at station 152.

These surface water trends of the major nutrients are summarized in Fig. 10. The low values north of ~59–60°S are in the PFZ and SAZ, and are largely due to mixing of temperate low-nutrient waters with polar high-nutrient waters, also judging from the similar values at 25 m and 50 m depth. The high values at and south of ~61°S are truly Antarctic. At ~68°S, the depletion of silicate and also nitrate at 25 m relative to 50 m depth is likely due to significant biological removal in the preceding spring and summer seasons. The recent existence of plankton blooms with downward transport of biogenic matter is supported by the observation during our cruise of a strong deficiency of ^{234}Th (Fig. 10). Previously in the austral spring of 1992 plankton blooms were reported in exactly the same region (Boyd et al., 1995; Savidge et al., 1995).

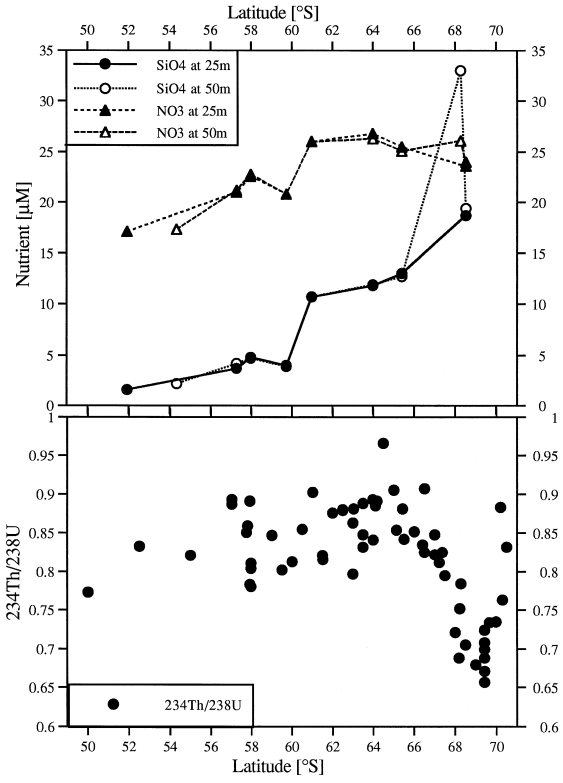

Fig. 10. The lateral distributions of nitrate (μM) and silicate (μM) in the samples at 50 m depth. Also shown the surface water deficiency of total (dissolved + particulate) ^{234}Th vs. radioactive parent ^{234}U, where the low ratios at about 68°S are due to recent removal of ^{234}Th in plankton blooms.

3.3. Diatom abundance and chlorophyll a

The phytoplankton species distribution was reported by van Leeuwe (1997) and van Leeuwe et al. (1998a). At all stations there was a very low background population of various prymnesiophytes, green algae, cyanobacteria en dinoflagellates. Diatoms were found only at stations south of the Polar Front where they often dominated the algal biomass (Fig. 11). The diatom distribution closely reflects the surface water concentrations of dissolved silicate, where at lower ambient surface water values of 2–3 μM silicate north of the Polar Front (Fig. 10) no diatoms were found either.

The ambient levels of Chl *a* were found to vary somewhat but were generally very low at concentrations ranging from 30 to 150 ng l^{-1} in the upper 100 m (Fig. 12). At most stations, values were low at about 40 to 80 ng l^{-1} (e.g., stations 37, 154 and 135 in Fig. 12). At or just south of the Polar Front at

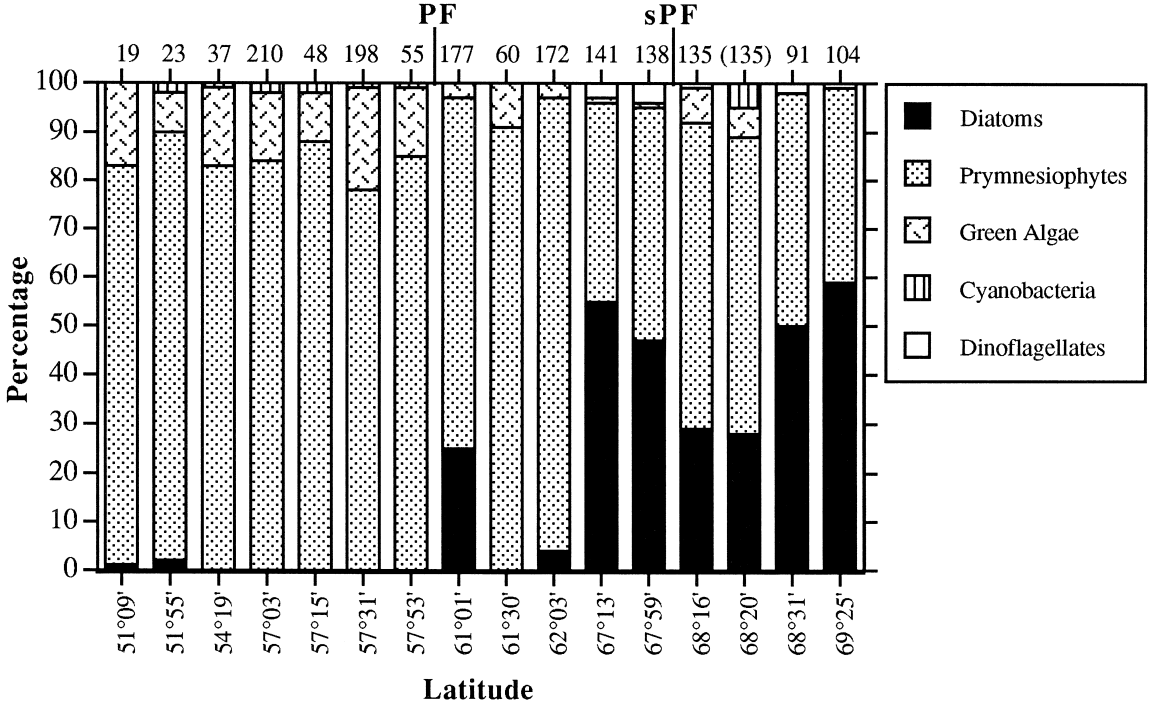

Fig. 11. The percentual species distribution of major taxonomic groups of phytoplankton at 16 stations ranked according to increasing latitude [°S] at lower horizontal axis. Note the positions of the Polar Front (PF) and southern Polar Front (sPF). See upper horizontal axis for corresponding station numbers as in Table 2. Additional hydrocast of station (135) in brackets slightly more southerly at 68°20′S due to ships drift. Drawn after findings of the parallel investigation by van Leeuwe et al. (1998a), see their Table 1. The shown relative abundances are based on a combination of flow cytometric cell counts, microscopic cell counts and HPLC analyses of photopigments characteristic for certain taxonomic groups, see further in (van Leeuwe et al., 1998a).

station 177 somewhat higher Chl *a* at ~ 125 ng l^{-1} together with Phaeophorbide breakdown products of Chl *a* constitute an inventory of ~ 150 ng l^{-1} as evidence of preceding and ongoing elevated biological activity. This might suggest the Polar Front to be more favorable for plankton growth, as observed more distinctly elsewhere (de Baar et al., 1995; Bathmann et al., 1997). However, the station 162 in the open southern ACC also shows elevated Chl *a* very similar at ~ 125 ng l^{-1}, thus the Polar Front (St. 177) hardly stands out as a biological more productive site.

The highest concentrations of Chl *a* were found near the Southern Polar Front (sPF) at about 68–69°S. There, ~ 160 ng l^{-1} was observed in the upper 90 m of station 91 (Fig. 12). The higher concentrations at ~ 50 ng l^{-1} of Phaeophorbides, in combination with the overall ~ 250 ng l^{-1} inventory of Chl *a* + Phaeo, and the deficiencies of silicate, nitrate and ^{234}Th (Fig. 10) hint at preceding blooming of diatoms, with export of biogenic particles out of the euphotic zone. Even higher concentrations of Chl *a* at ~ 200 ng l^{-1} were found in the upper 50 m at nearby station 104 (69°25′S, 94°10′W, not shown).

When integrated over the complete water column, the inventories of Chl *a* (mg m^{-2}) and Phaeophorbides are generally very low at 10–15 and 5–10 mg m^{-2}, respectively (Fig. 13), with considerable variability such that frontal zones no longer stand out as more productive sites.

3.4. Dissolved Fe

At all stations the dissolved Fe (< 0.4 μ) was determined (Fig. 14). In the subsurface depth range

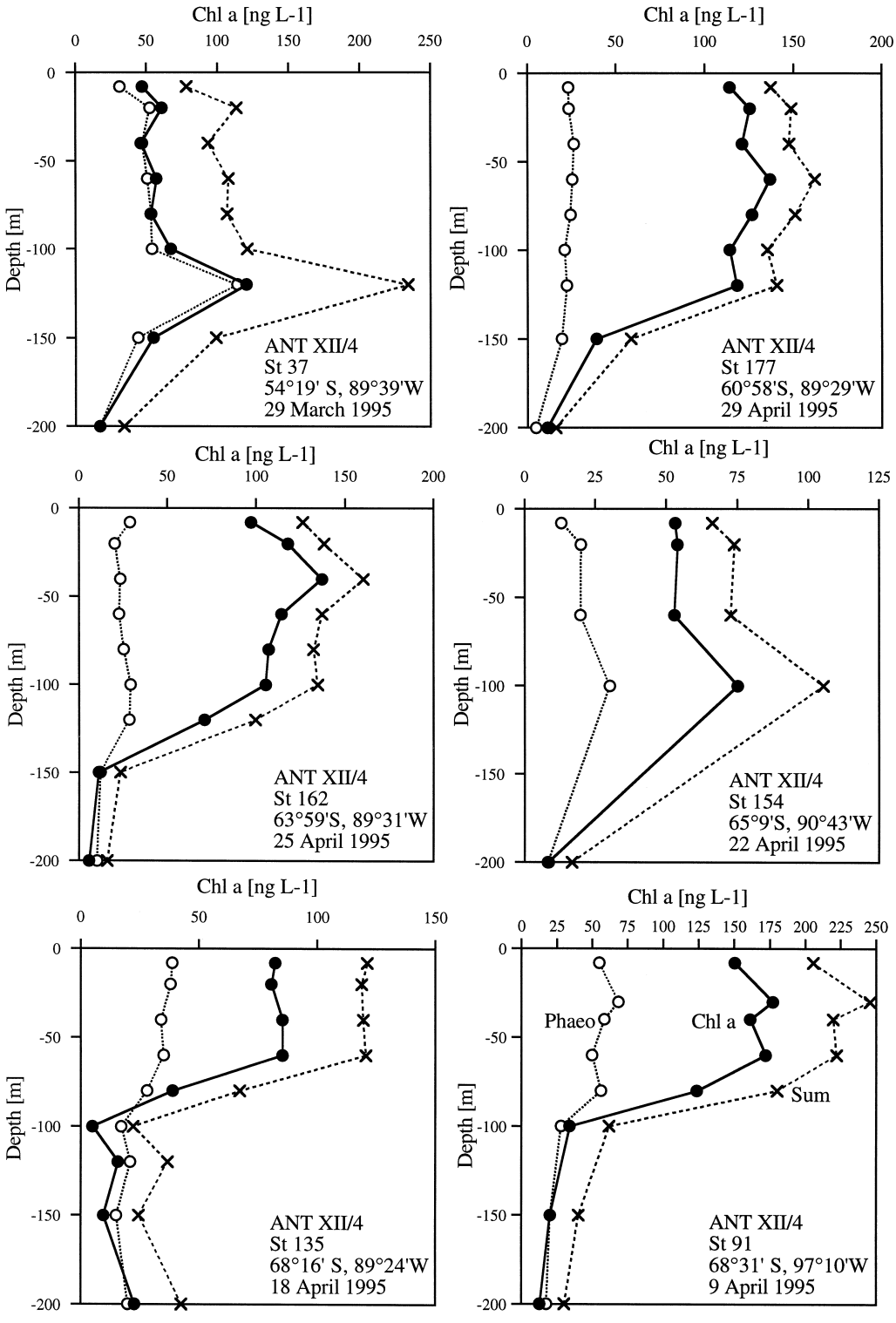
Chl a [ng L-1]
Depth [m]
ANT XII/4
St 37
54°19' S, 89°39'W
29 March 1995
ANT XII/4
St 177
60°58'S, 89°29'W
29 April 1995
ANT XII/4
St 162
63°59'S, 89°31'W
25 April 1995
ANT XII/4
St 154
65°9'S, 90°43'W
22 April 1995
ANT XII/4
St 135
68°16' S, 89°24'W
18 April 1995
Phaeo
Chl a
Sum
ANT XII/4
St 91
68°31' S, 97°10'W
9 April 1995

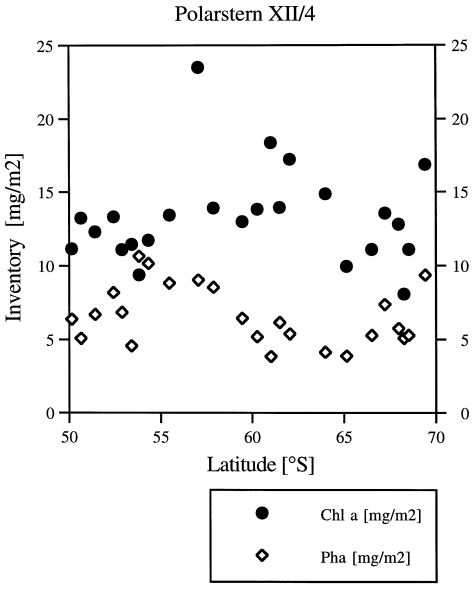

Fig. 13. Integrated Chl *a* (mg m^{-2}) and Phaeophorbides (mg m^{-2}) in the water column for all 24 stations along 90°W where these variables were measured.

of 100–400 m the concentrations were quite uniform around 0.2 to 0.3 nM but occasional higher and lower values were found. In the deeper range of 400–800 m, similar concentrations of 0.2–0.3 nM prevail, with some notable enhancements to 0.40–0.47 nM at station 199, which is situated in the Polar Frontal Zone (PFZ), and southernmost stations 135 and 91 at or near the sPF and CWB, where deeper waters may become affected by some input from continental margin sediments. At station 199, the total dissolvable Fe also tends to be higher at 400–800 m than at 100–400 m depth, but this can hardly be compared with the other stations due to lack of data (Table 1). At station 177 (60°58′S, 89°29′W), the dissolved Fe is extremely low at about 0.1–0.2 nM in the upper 100 m of the water column, with minimum concentrations of 0.05 nM in the upper 50 metres. The lower values at about 0.1 nM appear to be mostly at stations 48 (57°16′S, 91°14′W), 199 (57°58′S, 91°51′W), 177 (60°58′S, 89°29′W), 162 (63°59′S, 89°31′W) and 152 (65°24′S, 91°10′W) but are also found at most nearshore site 91 (68°31′S, 97°10′W). In contrast with the major nutrients (Fig. 10) there hardly is a latitudinal trend for trace nutrient Fe in surface waters, except for a tendency to somewhat higher values in the northernmost subantarctic waters of stations 37 and 48. For the stations 135 and 91 in the Bellingshausen Sea (Fig. 14) the enhanced Fe in deeper waters suggest some continental input, but in surface waters sampled in autumn this has disappeared, likely due to uptake and removal by recent blooms in spring and summer. This and previous Southern Ocean data as discussed below does now provide a glimpse on spatial distribution (Fig. 9d). On the other hand the seasonality of dissolved Fe has hardly been investigated in Antarctic surface waters.

3.5. Total dissolvable Fe

At three stations some or all sampling depths were also analyzed without filtration (Table 1). The resulting total dissolvable Fe is generally up to twofold higher than the dissolved Fe at the same depth (Fig. 14). At stations 199, 162 as well as 177 the dissolved Fe < 0.4 μ is well below the total dissolvable Fe values, as one would expect. This consistent trend further confirms the reliability of applied filtration procedures.

4. Discussion

4.1. Dissolved Fe

The dissolved Fe concentrations are averaging at 0.25 ± 0.14 nM ($n = 84$) with excursions to lower

Fig. 12. The vertical distribution of Chl *a* (ng l^{-1}) in the upper 200 m of the water column (filled dots) at 6 of the 24 stations where measurements were made, the selected 6 being stations where Fe was also measured. Also shown the Phaeophorbides (ng l^{-1}) which are breakdown products of Chl *a* due to zooplankton grazing and deemed to be somewhat indicative of preceding bloom conditions (open dots). Crosses represent the sum of Chl *a* and Phaeophorbides. Note the ng l^{-1} units (10^{-9} g l^{-1}) for these very low abundances.

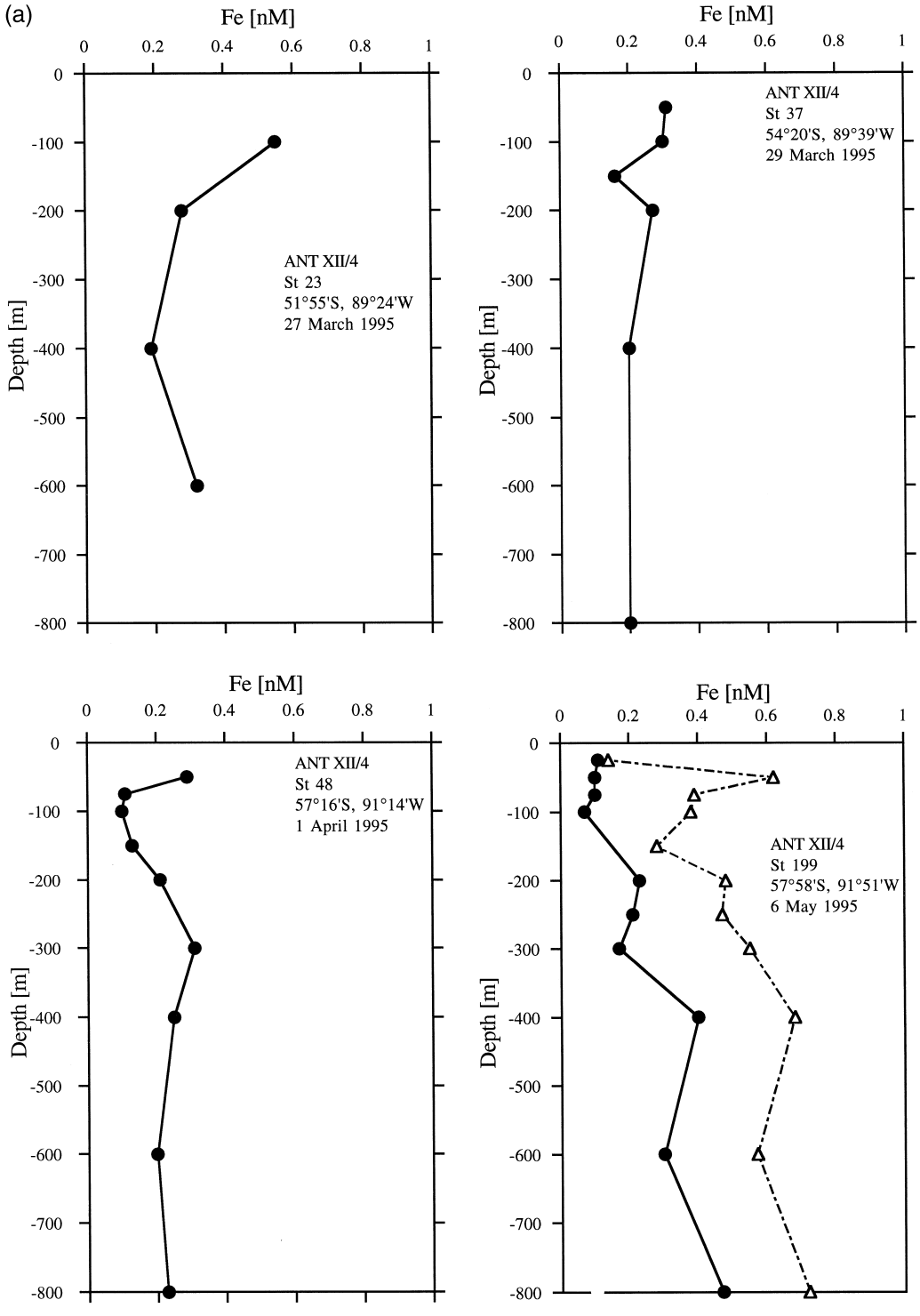
(a)
Fe [nM]
0 0.2 0.4 0.6 0.8 1
Depth [m]
0 -100 -200 -300 -400 -500 -600 -700 -800
ANT XII/4
St 23
51°55'S, 89°24'W
27 March 1995
ANT XII/4
St 37
54°20'S, 89°39'W
29 March 1995
ANT XII/4
St 48
57°16'S, 91°14'W
1 April 1995
ANT XII/4
St 199
57°58'S, 91°51'W
6 May 1995

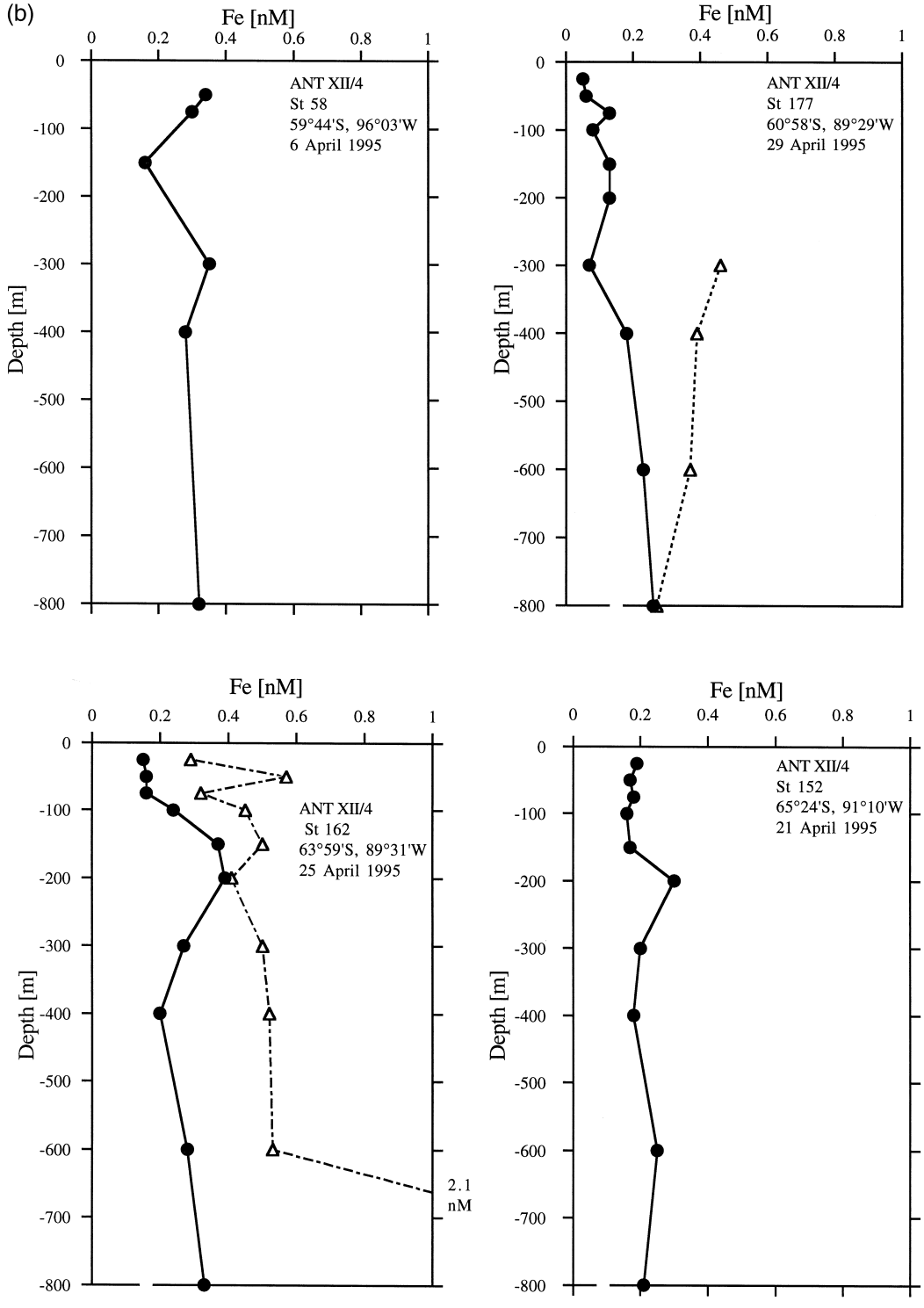
(b)
Fe [nM]
Depth [m]
ANT XII/4
St 58
59°44'S, 96°03'W
6 April 1995
ANT XII/4
St 177
60°58'S, 89°29'W
29 April 1995
ANT XII/4
St 162
63°59'S, 89°31'W
25 April 1995
2.1
nM
ANT XII/4
St 152
65°24'S, 91°10'W
21 April 1995

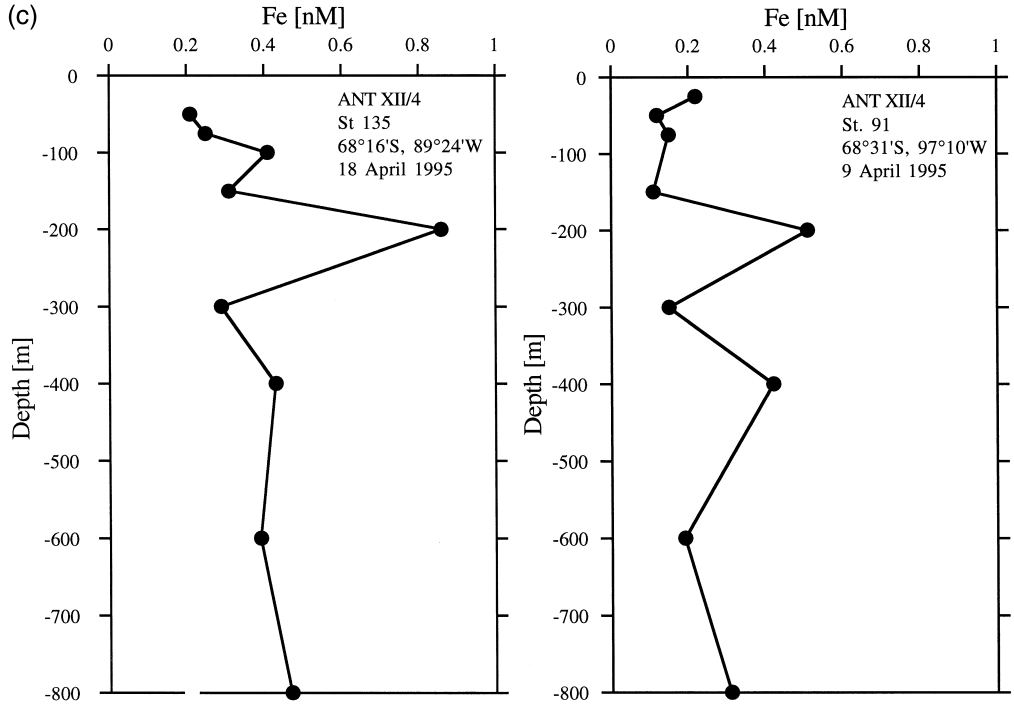

Fig. 14. Vertical profiles of dissolved Fe (nM) in the fraction filtered over 0.4 μ nominal pore size membrane filters (filled dots). Also shown for some stations are the total dissolvable Fe (nM) in unfiltered seawater (open triangles).

(0.05 nM) as well as higher (0.55 nM, 0.86 nM) values. The tendency to lower values in surface waters is reflected in a slightly lower mean value of 0.21 ± 0.14 nM ($n = 41$) in the upper 150 m only, as compared to 0.29 ± 0.13 nM ($n = 43$) in the underlying 150–800 m depth interval. The very surface waters (0–50 m) have a lower mean value again of 0.16 nM ($n = 14$).

The slight enhancement at the PFZ is reminiscent of the better documented and much larger enhancement found at 6°W at the Atlantic Polar Front (de Baar et al., 1995; Löscher et al., 1997). Latter values of dissolved Fe were averaging at 1.87 nM decreasing to 1.14 nM within three weeks of the ongoing spring season. However, at 90° W in the remote Pacific any upstream sources of Fe in coastal margin sediments or upwind supply by land-derived aeolian input are further away. Also in austral autumn, about 4–5 months later in the season, the smaller input of Fe, in itself, may have become further depleted by biological removal.

The minima of 0.05 nM, or in fact all values lower than 0.1 nM, are the lowest reported thus far for the Southern Ocean, confirming the expectation for this most remote part of the Southern Ocean. For example Löscher et al. (1997), report a minimum value of 0.17 nM at 54°S, 6°W in the Atlantic region of the southern ACC (sACC) where surface waters were on average 0.48 nM decreasing to 0.31 nM within 3 weeks of increasing spring season. In the Drake Passage, dissolved Fe was found to range from 0.1 to 0.26 nM in surface waters (30–300 m) and 0.50–0.76 nM at 550–1450 m intermediate depths (Martin et al., 1990a,b; when ignoring rejected values in the 0.52–1.55 nM range). In sub-Antarctic surface waters southwest of Tasmania, minimum dissolved (< 0.2 μ) concentrations were at 0.1–0.29 nM (45–53°S, 140°W) in the upper 100 m with higher values at ~ 0.2–0.3 nM at greater depths of ~ 50–400 m (Sedwick et al., 1997). The tendency to elevated dissolved Fe (0.31–0.76 nM) at their other stations towards the Antarctic continent is

consistent with the higher dissolved Fe reported previously for the Weddell–Scotia Confluence region downstream the Peninsula (Nolting et al., 1991), the semi-enclosed Weddell Sea (Westerlund and Öhman, 1991), the inshore Gerlache Strait (Martin et al., 1990a) and in the subsurface (> 100 m) at our southernmost stations 135 and 91 towards the Antarctic continent (Figs. 9d and 14).

Thus, both the range (0.05–0.85 nM) and mean value (0.25 nM) at our section are below values elsewhere in the Southern Ocean. This is even more true for the upper 50 m with a mean value of 0.16 nM and overall confirms the original expectation. However, the difference with other Antarctic sectors (longitudes) is not very dramatic and this most remote Pacific area of the Southern Ocean still exhibits discernible Fe values. This may be reflected upon both in terms of place and of time. At any given longitude the Antarctic Circumpolar Current is known to be quite homogenous in hydrography and nutrient contents throughout the water column, and this now appears more or less the case for dissolved Fe as well. The underlying mechanism may well be the more intense exchange with surface sediments, due to the very high kinetic energy of the ACC as discussed below. Within the time domain one realizes our dataset was collected in late summer to early autumn. On the one hand depletion of the nutrient Fe would therefore be expected, due to summer stratification and concomitant biological removal. On the other hand the deep mixed layers (Fig. 7) may already have eradicated any such conceivable summer signal of surface water depletion of dissolved Fe.

The minimum values of 0.05 nM here reported for the Southern Ocean are comparable to minima in the open North Pacific Ocean where lowest values of 0.05–0.08 nM (Martin and Gordon, 1988) were found in the centre of the basin (35.8°N, 122.6°W) and more towards the east (35.1°N, 128.2°W; 33.3°N, 139.1°W). An even lower minimum value of dissolved (< 0.3 μ) Fe at 0.02 nM was observed in the summer (July 1983) in subsurface waters some 200 km north off Hawaii (28°N, 155°W; Bruland et al., 1994). At nearby station ALOHA (22°45′N, 158°W) in the winter season (January 1994) the dissolved (< 0.2 μ) Fe was somewhat higher at 0.17–0.24 nM in surface waters, with a minimum of 0.09 nM at 160 m depth (Rue and Bruland, 1995). In the Northeast Atlantic Ocean in spring and summer the ambient dissolved Fe in the euphotic zone was about 0.07–0.23 nM at 47°N, 20°W and 0.08–0.12 nM at 59°N,20°W (Martin et al., 1993). At both Atlantic sites, the dissolved Fe steadily increased with depth.

In the temperate northwest Atlantic Ocean, Wu and Luther (1994) found dissolved Fe < 1 nM in surface waters. In autumn (October 1991), the surface waters were very depleted of Fe leading to an overall nutrient-type profile increasing from 0.2 nM at the surface to 0.9 nM at 1000 m depth. Yet in mid-summer (July 1992) the dissolved Fe was higher at 0.6 nM in the surface waters compared to a subsurface minimum of 0.2 nM at 50 m depth and then increasing again to 0.7–0.8 nM at 1000 m depth. Such seasonality of dissolved Fe is to be expected in surface waters elsewhere, due to seasonal input as well as seasonal biological activity deemed to be largely responsible for Fe removal. In general high latitudes experience more seasonality than temperate and low latitudes, and this likely is reflected in seasonal changes of Fe concentrations and biological activity in the Southern Ocean (e.g., spring evolution, de Baar et al., 1995).

Finally, in the northwestern Indian Ocean, during the northeast monsoon, the surface water concentrations of dissolved Fe were 0.15 to 0.47 nM, and rapidly increased with depth to 5.16 nM in low-oxygen waters at 200 m depth (Takeda et al., 1995). Latter values are comparable to those reported by Saager et al. (1989) for one station in the same region, apart from improved reproducibility of the more recent data of Takeda et al. (1995).

4.2. Total dissolvable and particulate Fe

The total dissolvable Fe values are about twice the dissolved values, suggesting that the Fe is roughly equally distributed between the dissolved and particulate phases. The difference between total dissolvable and dissolved Fe is the apparent particulate Fe. For the upper water column (< 100 m), this particulate fraction may partly be due to plankton matter. However, the abundance of plankton is low judging from the ambient Chl *a*. levels of about 100 ng l^{-1} at sites near station 199 (not shown) and ~ 125 ng

l^{-1} at station 162 (Fig. 12). In the deeper waters (> 150 m) the apparent particulate Fe is largely ascribed to mineral particles originating from both the underlying deep seafloor and adjacent continental margin sources. The Antarctic Circumpolar Current extends throughout the whole vertical water column and moreover has a very high kinetic energy compared to deep water masses in other oceans (see Löscher et al., 1997; their Fig. 8). This and the general upwelling regime of the ACC may give rise to some re-suspension of sedimentary particles which would be the most likely explanation for the apparent particulate Fe of ~0.2–0.3 nM.

These values of total dissolvable Fe are again comparable to the ~0.4–0.8 nM at two subantarctic stations southwest of Tasmania (40°–53°S; 140°W; Sedwick et al., 1997). At their next stations (40°S, 140°W and 41°S, 143°33′W) the total dissolvable Fe was in the same ranges, except for a few values of ~1.2 nM at greater depths consistent with the closer proximity of the continental margins off Tasmania/Australia. In the Atlantic region the ACC exhibits total dissolvable Fe in the ~0.6–2.0 nM range at both sides of the Polar Front, with appreciably higher values such as 4–5 nM within the Polar Front itself (Löscher et al., 1997). In deeper Atlantic waters of the ACC the total dissolvable Fe was found to be in the 1–3 nM range, with higher values in the Antarctic Bottom Water (AABW) consistent with its Weddell Sea source regions (Westerlund and Öhman, 1991; Nolting et al., 1991). In the Indian sector of the Southern Ocean the total dissolvable Fe was found to be in the 0.4–6.2 nM range in the upper 250 m of the water column at stations extending from 49° to 66°S at the 62°E meridian (Sarthou et al., 1997), and similar in value as the dissolved Fe (filtered) at the same sites (Sarthou, unpublished results). In the northwest Atlantic total dissolvable Fe values were found to range from 0.7 to 2.1 nM in the upper 1000 m of the water column (Wu and Luther, 1994).

4.3. Limitation of the phytoplankton community

Throughout the region the ambient dissolved Fe was very low and phytoplankton biomass extremely low, with a conspicuous absence of blooms (defined as Chl $a > 1$ μg l^{-1} = 1000 ng l^{-1}). The very deep wind mixed layers often exceeding 100 m (Fig. 7) obviously are detrimental for a stable light climate, as required for any appreciable development of phytoplankton biomass (Lancelot et al., 1993; de Baar and Boyd, 1999). However, the low dissolved Fe ~0.2 nM is also deemed to be severely limiting for all algae. Here, one realizes that Fe plays a key role in the functioning of the photosystems of the plant cell, i.e., stress by light and Fe are not independent factors. Rather, they are reinforcing one another as growth limitations (van Leeuwe, 1997).

The complementary investigations by Timmermans et al. (1998), using bioassays under more optimal light of highly Fe-stress sensitive physiological indicators nitrate reductase, ^{15}N-nitrate assimilation and flavodoxin, have shown that the complete indigenous phytoplankton community is Fe-stressed. This was further confirmed by van Leeuwe et al. (1998b) observing a decrease of fluorescence upon experimental Fe addition, the fluorescence deemed indicative of poor functioning of photosystem II due to Fe deficiency in the electron transport systems (Behrenfeld et al., 1996). Thus, Fe-stress not only severely restricts the larger microphytoplankton, but also the nanophytoplankton and picophytoplankton as part of the small foodweb are Fe-stressed. In other Antarctic regions and seasons, massive blooms of larger microphytoplankton such as Phaeocystis (Smith et al., 1996) and large diatoms have been observed (Jochem et al., 1995; Bathmann et al., 1997; Quéguiner et al., 1997), where ample availability of dissolved Fe (de Baar et al., 1995; Löscher et al., 1997; van Leeuwe et al., 1997) as well as an improved light climate (Jochem et al., 1995), were found to play a key role.

The unfavorable combination of low Fe and poor light climate were reflected in the low abundance of phytoplankton biomass (Figs. 12 and 13). Cell numbers as determined by flow cytometry were also very low (van Leeuwe et al., 1998a). At three stations around 57°S well north of the SubAntarctic Front (SAF) the cell numbers were averaging between 5000–7000 cells ml^{-1}. At truly Antarctic stations south of the Polar Front the numbers of cells were lower at about 3000 cells ml^{-1}, but for the southernmost stations at ~68°S near the southern Polar Front (sPF) there existed an additional population of

large diatoms (Fig. 11) which cannot be detected by flow cytometry. This nicely coincided with the higher levels of Chl *a* (Fig. 12) and the stronger deficiencies of major nutrients and ^{234}Th (Fig. 10) all indicative of recent diatom blooms. Most notably the shallower mixed layer depths observed at some of these stations (e.g., site 135 in Fig. 7) also is favorable for growth of all phytoplankton species. High numbers of the large diatom *Fragilariopsis kerguelensis* were reminiscent of its even higher abundances in the Atlantic Polar Front (de Baar et al., 1997a) as result of enhanced Fe supply (de Baar et al., 1995; Löscher et al., 1997). Similarly various *Chaetoceros* species and some other diatom taxonomic groups were also present at the sPF sites.

4.4. The role of diatoms

The floristic composition of the plankton community was further delineated using photopigments as taxonomic indicators (van Leeuwe et al., 1998a). At all subAntarctic sites diatoms were virtually absent, presumably due to the low ambient silicate at $\sim$ 2–4 nM preventing diatom growth. In the published literature one finds that in cultures and natural assemblages of large diatoms the half-saturation constants K_m for growth appears to range from about 0.4 to 5 μM silicate. Brzezinski and Nelson (1996) reckon that 2.3 μM is the representative value for temperate oceanic species. Previously silicate limitation has been described for Antarctic diatom blooms in the Ross Sea and the endemic diatoms showed higher K_m values of about 5 μM, whereas even higher K_s of 12–22 μM have also been reported for Antarctic diatoms (Jacques, 1983; Sommer, 1986). Thus silicate limitation in itself may explain the virtual absence of diatoms at our subAntarctic stations.

In the absence of diatoms, the subAntarctic stations were dominated by small flagellate algae, notably Prymnesiophyceae (78–93%) and green algae (7–18%) were dominating (van Leeuwe et al., 1998a). Nevertheless, their absolute numbers and biomass were low, likely due to Fe stress, poor light climate as well as grazing losses. Cyanobacteria represented only 1–2% of the biomass. This appears consistent with laboratory experiments showing that prokaryotes have about a tenfold higher Fe requirement than eukaryotes (Brand, 1991). However, due to their generally small size, their high specific surface would allow sufficient uptake of ambient Fe even when concentrations are low. Alternatively, it has been suggested that cyanobacteria grow poorly at low ambient temperatures, although their existence in polar waters has previously been reported (Gradinger and Lenz, 1989; Lételier and Karl, 1989; Andreoli et al., 1993; Detmer and Bathmann, 1997).

Within the Antarctic Ocean proper, the diatoms represent 25% of the biomass at station 177 just south of the Polar Front, then increase to 28–59% at the other Antarctic stations, the highest 59% diatoms being found at the southernmost station 103/104 on the sPF. At this site (St. 103 at 69°24′S, 95°01′W) the upper mixed layer was very shallow at about 40 m depth (not shown) thus providing favorable light conditions for diatom growth. A similar shallow mixed layer of 50 m at station 135 would also favor diatom growth. Even with the somewhat deeper mixed layer of 90 m at site 91 a rather high abundance of Chl a (Fig. 12) is largely consistent with dominance by diatoms (Fig. 11). Thus, it appears the diatoms are more or less superimposed on a quite uniform background population of the four other major taxa. As a result, the Prymnesiophytes and green algae contribute only about 40–63% and 1–9% of the biomass at these sites, with another minor amount of 1–4% dinoflagellates (Fig. 11). Clearly in these silicate-rich Antarctic waters, the diatoms have equal opportunity for growth as the other algae, but all remain to be limited severely by low ambient Fe and deep wind-mixed layers. This being said the higher standing stock of diatoms at the sPF site along with its silicate depletion (Fig. 10) suggests that the diatoms had been able to respond quickly to an enhanced supply of Fe by the sPF in the period just before our cruise. At the time of occupation of these stations, most surface water Fe had already been removed and we observed only the remnants of a bloom and the deficiencies of nutrients and ^{234}Th (Fig. 10). The dimensionless activity ratio ^{234}Th/^{238}U is a transient variable, where values below 1 are ^{234}Th deficiencies due to scavenging removal on settling biogenic particles. Because of the continuous production from decay of ^{238}U and subsequent decay with 24.1 days halflife of ^{234}Th any deficiency can only be ascribed to removal

within the preceding period in the order of 1–2 months. Thus the observed ^{234}Th deficiency at about 69°S (Fig. 10) is clear evidence for the existence of a bloom in the preceding summer period.

4.5. Iron, silicate, light, diatom blooms and global element budgets

In a recent review of all Fe-phytoplankton studies done thus far in the world oceans, de Baar and Boyd (1999) found a strikingly consistent response to Fe enrichment. Whether the enrichment was natural or experimental, in all published cases in all HNLC waters of all oceans the major response was a rapid increase of larger bloom-forming diatoms. The few cases where the overall biomass response to Fe addition was disappointing (e.g., Martin et al., 1993) were found to correspond with those HNLC waters where nitrate and phosphate were abundant but silicate was depleted (de Baar and Boyd, 1999), i.e., diatoms were not able to respond to Fe addition. The virtual absence of diatoms in the HNLC subAntarctic waters of our study is consistent with this notion of combined limitation by Fe and silicate of diatom blooms. In the HNLC waters south of the Polar Front, there is plenty silicate but still Fe deficiency prevents diatoms from blooming. Throughout the complete section, the other algae cannot bloom due to Fe stress as well, and due to their generally smaller size would also suffer more grazing losses. Thus, the common Prymnesiophyte *Phaoecystis* sp. cannot form the massive blooms as commonly observed in presumably more Fe-rich, semi-enclosed waters of the Ross Sea (Smith et al., 1996).

The remnants of diatom blooms at the sPF, the previous observations of large diatom blooms at this sPF some months earlier in the season (Boyd et al., 1995; Savidge et al., 1995), as well as the Fe-stimulated diatom blooms at the Atlantic Polar Front (de Baar et al., 1995, 1997a) all hint at diatoms as very opportunistic species being able to respond very quickly to a seasonal or occasional Fe input. This rapid wax and wane of diatom blooms appears to be an intrinsic period of the overall life cycle strategy, where initial vegetative reproduction in early bloom stages is followed by sexual reproduction and massive shedding of diatom frustules at the end of the bloom (Crawford, 1995; Crawford et al., 1997). These diatom blooms are major vehicles for drawdown of CO_2 from the atmosphere (Robertson and Watson, 1995; Bellerby et al., 1995; Bakker et al., 1997) as well as export of organic particles into the deep sea (^{234}Th in Fig. 10; Rutgers van der Loeff et al., 1997). This appears true not only for the Antarctic Ocean, but also for other HNLC regions where silicate is abundant (equatorial and subArctic Pacific). In addition in temperate waters of for example the North Atlantic Ocean the first stabilization of the surface waters very early in spring allows the rapid utilization to depletion of the winter values of silicate, accompanied by CO_2 drawdown and particle export into deep waters.

In temperate waters of the North Atlantic Ocean and elsewhere the classical spring bloom is well understood. There upon the first stabilization of the water column due to lower wind stress, as well as the seasonal increase of insolation, the winter values of major nutrients silicate, nitrate and phosphate rapidly become removed. For spring and summer blooms in the Antarctic Ocean we now envision a similar scenario, but now Fe is the limiting nutrient as the major nutrients remain in excess throughout the spring and summer season. Thus, in frontal regions like the Atlantic PF (de Baar et al., 1995) and the Bellingshausen sPF (Boyd et al., 1995; Savidge et al., 1995) and nearshore neritic waters (de Baar et al., 1990; Buma et al., 1991; Nolting et al., 1991), the Fe supply is adequate, and one encounters spring and summer blooms once the light climate has become more favorable. This leads to rapid removal of Fe over several weeks time (de Baar et al., 1995; Löscher et al., 1997) and later in the season or in autumn (sPF in our study) only remnants of summer blooms can be found. The optimal light climate is in Austral summer when insolation is highest and wind stress minimal (Trenberth et al., 1990), but quite often the supply of Fe may already have been depleted in the preceding spring bloom. On the other hand in remote areas like the remaining part of our research section, the annual supply of Fe is so very low that even in spring and summer blooms can hardly develop.

From the above mentioned and various other studies (Stoll et al., 1996a,b), it now becomes apparent

that the uptake of atmospheric CO_2 by the oceans is strongly dominated by biological processes in plankton blooms. Here, diatom blooms and their regulation by availability of silicate, Fe and light appear to play the key role. Thus, towards understanding and quantification of the uptake of fossil fuel CO_2 by the oceans (Houghton et al., 1996), as well as the function of Fe in the ocean carbon cycle, it is recommended that diatoms, their physiology, life cycle and nutrient requirements, will become the focus of future research.

Acknowledgements

This research is part of the JGOFS Southern Ocean Program and was done during the ANT XII/4 Leg of the RV Polarstern. We are grateful to chief scientist Dr. Rainer Gersonde (AWI, Alfred Wegener Institute for Polar and Marine Research, Bremerhaven), other shipboard colleagues, captain, officers and crew for kindly accomodating our research. Nutrient values were provided by Jan van Ooyen (NIOZ) and the shipboard Chl a studies were done by M. Templin (AWI). As in previous work (de Baar et al., 1990; Buma et al., 1991; de Baar, 1994; Löscher et al., 1997; de Baar and Boyd, 1999) an effort was made to acknowledge without bias all relevant published work by other laboratories. This is deemed essential as to provide a complete presentation of existing facts and knowledge to the readership, for the latter to be able to decide themselves on the validity of data and interpretations. This research was supported by grants from the Netherlands Antarctic Programme (NAAP) under the Netherlands Organization for Scientific Research (NWO), by the project Marine Ecosystems Regulation: Trace Metal and Carbon Dioxide Limitations (MERLIM) of the European Union within the Marine Science and Technology Program under Contract No: MAS3-CT95-0005, and by the project Carbondioxide Uptake in the Southern Ocean (CARUSO) of the European Union within the Climate and Environment Programme under Contract No: ENV4-CT97-0472. This is NIOZ contribution number 3230 and AWI contribution number 1434.

References

Andreoli, P.C., Scarabel, L.R., Tolomio, C., 1993. Distribution du picoplankton photoautotrophe dans la baie de Terra Nova (Mer de Ross, Antarctique) pendant l'eté austral 1989–1990. Algological Studies 68, 123–132.

Bakker, D.C.E., de Baar, H.J.W., Bathmann, U.V., 1997. Changes of carbon dioxide in surface waters during spring in the Southern Ocean. Deep-Sea Research II 44, 91–128.

Bathmann, U.V., Smetacek, V., de Baar, H., Fahrbach, E., Krause, G., 1994. In: The expeditions ANTARKTIS X/6-8 of the Research Vessel 'POLARSTERN' in 1992/1993. 236 pp. Berichte zur Polarforschung, 135.

Bathmann, U., Scharek, R., Dubischar, C., Klaas, C., Smetacek, V., 1997. Chlorophyll and phytoplankton species distribution in the Atlantic sector of the Southern Ocean in spring. Deep-Sea Research II 44, 51–68.

Behrenfeld, M.J., Bale, A.J., Kolber, Z.S., Aiken, J., Falkowski, P., 1996. Confirmation of iron limitation of phytoplankton photosynthesis in the equatorial Pacific Ocean. Nature 383, 508–511.

Bellerby, R.G.J., Turner, D.R., Robertson, J.E., 1995. Surface pH and pCO2-distributions in the Bellingshausen Sea, Southern Ocean, during early austral summer. Deep-Sea Research II 42, 1093–1107.

Boyd, P.W., Robinson, C., Savidge, G., Williams, P.J., Le, B., 1995. Water column and sea-ice primary production during Austral spring in the Bellingshausen Sea. Deep-Sea Research II 42, 1177–1200.

Brand, L.E., 1991. Minimum iron requirements of marine phytoplankton and the implications for the biogeochemical control of new production. Limnology and Oceanography 36, 1756–1771.

Bruland, K.W., Orians, K.J., Cowen, J.P., 1994. Reactive trace metals in the stratified central North Pacific. Geochim. Cosmochim. Acta 58, 3171–3182.

Brzezinski, M.A., Nelson, D.M., 1996. Chronic substrate limitation of silicic acid uptake rates in the western Sargasso Sea. Deep-Sea Research II 43, 437–453.

Buma, A.G.J., de Baar, H.J.W., Nolting, R.F., van Bennekom, A.J., 1991. Metal enrichment experiments in the Weddell-Scotia Seas: effects of iron and manganese on various plankton communities. Limnology and Oceanography 36, 1865–1878.

Chen, J.H., Edwards, L.R., Wasserburg, G.J., 1986. ^{238}U, ^{234}U and ^{232}Th in seawater. Earth Planet. Sci. Lett. 80, 241–251.

Comiso, J.C., McClain, C.R., Sullivan, C.W., Ryan, J.P., Leonard, C.L., 1993. Coastal zone color scanner pigment concentrations in the Southern Ocean and relationships to geophysical features. J. Geophys. Res. 98, 2419–2451.

Crawford, R.M., 1995. The role of sex in the sedimentation of a marine diatom bloom. Limnology and Oceanography 40, 200–204.

Crawford, R.M., Hinz, F., Rynearson, T., 1997. Spatial and temporal distribution of assemblages of the diatom *Corethron criophilum* in the Polar Frontal region of the South Atlantic. Deep-Sea Research II 44, 479–498.

de Baar, H.J.W., 1994. von Liebig's Law of the minimum and plankton ecology (1899–1991). Progress in Oceanography 33, 347–386.

de Baar, H.J.W., Boyd, P.M., 1999. The role of iron in plankton ecology and carbon dioxide transfer of the global oceans. In: Hanson, R.B., Ducklow, H.W., Field, J.G. (Eds.), The Dynamic Ocean Carbon Cycle: A Midterm Synthesis of the Joint Global Ocean Flux Study, Chap. 4. International Geosphere Biosphere Programme Book Series, Cambridge Univ. Press, in press.

de Baar, H.J.W., Buma, A.G.J., Jacques, G., Nolting, R.F., Tréguer, P.J., 1989. Trace metals—iron and manganese effects on phytoplankton growth. Berichte zur Polarforschung 65, 34–44.

de Baar, H.J.W., Buma, A.G.J., Nolting, R.F., Cadée, G.C., Jacques, G., Tréguer, P.J., 1990. On iron limitation of the Southern Ocean: experimental observations in the Weddell and Scotia Seas. Marine Ecology Progress Series 65, 105–122.

de Baar, H.J.W., de Jong, J.T.M., Bakker, D.C.E., Löscher, B.M., Veth, C., Bathmann, U., Smetacek, V., 1995. Importance of iron for phytoplankton spring blooms and CO2 drawdown in the Southern Ocean. Nature 373, 412–415.

de Baar, H.J.W., van Leeuwe, M.A., Scharek, R., Goeyens, L., Bakker, K.M.J., Fritsche, P., 1997a. Iron availability may affect the nitrate/phosphate ratio (A.C. Redfield) in the Antarctic Ocean. Deep-Sea Research II 44, 229–260.

de Baar, H.J.W., Gerringa, L., Jong, de, J.T.M., van Leeuwe, M.A., Nolting, R.F., Timmermans, K.R., Schoemann, V., 1997b. Iron and phytoplankton in the Pacific section of the Southern Ocean. Abstract Gordon Research Conference for Chemical Oceanography, New Hamsphire, August 1997.

de Jong, J.T.M., den Das, J., Bathmann, U., Stoll, M.H.C., Kattner, G., Nolting, R.F., de Baar, H.J.W., 1998. Dissolved iron at sub-nanomolar levels in the Southern Ocean as determined by ship-board analysis. Anal. Chim. Acta 377, 113–124.

Dehairs, F., Goeyens, L., Stroobants, N., Mathot, S., 1992. Elemental composition of suspended matter in the Scotia–Weddell Confluence area during spring and summer 1988 (EPOS Leg 2). Polar Biology 12, 25–33.

Detmer, A.E., Bathmann, U., 1997. Distribution patterns of autotrophic pico- and nanoplankton and their relative contribution to algal biomass. Deep-Sea Research II 44, 299–320.

Duce, R.A., Tindale, N.W., 1991. Atmospheric transport of iron and its deposition in the ocean. Limnology and Oceanography 36, 1715–1726.

Dugdale, R.C., Wilkerson, F.P., 1990. Iron addition experiments in the Antarctic: a re-analysis. Global Biogeochemical Cycles 4, 13–19.

Edwards, M.R., 1998. From a soup or a seed? Pyritic metabolic complexes in the origin of life. TREE 13 (5), 178–181.

Gordon, A.L., 1967. Structure of Antarctic waters between 20°W and 170°W. In: Bushnell, V.C. (Ed.), Antarctic Map Folio Series, Folio 6. American Geography Society, 10 pp.

Gordon, A.L., Molinelli, J., Baker, T.N., 1986. Southern Ocean Atlas. Columbia Univ. Press, New York, 1982; A.A. Balkema Publishers, Rotterdam, 1986.

Gradinger, R., Lenz, J., 1989. Picocyanobacteria in the high Arctic. Marine Ecology Progress Series 52, 99–101.

Gran, H.H., 1931. On the conditions for the production of plankton in the sea. Rapports et Proces verbaux des Réunions, Conseil International pour l'exploration de la Mer 75, 37–46.

Grashoff, K., Erhardt, M., Kremling, K., 1983. Methods in Seawater Analyses. Verlag Chemie, Weinheim, Germany, 419 pp.

Harvey, H.W., 1937. The supply of iron to diatoms. Journal of the Marine Biological Association of the United Kingdom 22, 205–219.

Helbling, E.W., Villafane, V., Holm-Hansen, O., 1991. Effect of iron on productivity and size distribution of Antarctic phytoplankton. Limnology and Oceanography 36, 1879–1885.

Holm-Hansen, O., Lorenzen, C.J., Holmes, R.W., Strickland, J.D.H., 1965. Fluorometric determination of chlorophyll. J. Cons. Perm. Int. Explor. Mer. 30, 3–15.

Houghton, J.T., Meira Filho, L.G., Callander, B.A., Harris, N., Kattenberg, A., Maskell, K., 1996. Climate Change 1995, The Science of Climate Change. Cambridge Univ. Press, Cambridge.

Hudson, R.J.M., Morel, F.M.M., 1990. Iron transport in marine phytoplankton: kinetics of cellular and medium coordination reactions. Limnology and Oceanography 35, 1002–1020.

Jacques, G., 1983. Some ecophysiological aspects of the Antarctic phytoplankton. Polar Biology 11, 315–328.

Jochem, F.J., Mathot, S., Quéguiner, B., 1995. Size-fractionated primary production in the open Southern Ocean in austral spring. Polar Biology 15, 381–392.

Kamykowski, D., Zentara, S.J., 1989. Circumpolar plant nutrient covariation in the Southern Ocean: patterns and processes. Marine Ecology Progress Series 58, 101–111.

Kumar, N., Anderson, R.F., Mortlock, R.A., Froelick, P.N., Kubik, P., Dittrich-Hannen, B., Suter, M., 1995. Increased biological productivity and export production in the glacial Southern Ocean. Nature 378, 675–680.

Landing, W.M., Haraldsson, C., Paxéus, N., 1986. Vinyl polymer agglomerate based transition metal cation chelating ion-exchange resin containing the 8-hydroxyquinoline functional group. Anal. Chem. 58, 3031–3035.

Lancelot, C., Mathot, S., Veth, C., de Baar, H.J.W., 1993. Factors controlling phytoplankton ice-edge blooms in the marginal ice-zone of the northwestern Weddell Sea during sea ice retreat 1988: field observations and mathematical modeling. Polar Biology 13, 377–387.

Lételier, R.M., Karl, D.M., 1989. Phycoerythrin-containing cyanobacteria in surface waters of the Drake Passage during February 1987. Antarctic Journal of the United States 24, 185–188.

Levitus, S., Conkright, M.E., Reid, J.L., Najjar, R.G., Mantyla, A., 1993. Distribution of nitrate, phosphate and silicate in the world oceans. Progress in Oceanography 31, 245–273.

Lewis, B.L., Landing, W.M., 1991. The biochemistry of manganese and iron in the Black Sea. Deep-Sea Research 38, 773–803.

Löscher, B.M., de Jong, J.T.M., de Baar, H.J.W., Veth, C., Dehairs, F., 1997. The distribution of iron in the Antarctic Circumpolar Current. Deep-Sea Research II 44, 143–188.

Martin, J.H., Fitzwater, S.E., 1988. Iron deficiency limits phytoplankton growth in the northeast Pacific subarctic. Nature 331, 341–343.

Martin, J.H., Gordon, R.M., 1988. Northeast Pacific iron distributions in relation to phytoplankton productivity. Deep-Sea Research 35, 177–196.

Martin, J.H., Gordon, R.M., Fitzwater, S.E., 1990a. Iron in Antarctic waters. Nature 345, 156–158.

Martin, J.H., Fitzwater, S.E., Gordon, R.M., 1990b. Iron deficiency limits phytoplankton growth in Antarctic waters. Global Biogeochemical Cycles 4, 5–12.

Martin, J.H., Gordon, R.M., Fitzwater, S.E., 1991. The case for iron. Limnology and Oceanography 36, 1793–1802.

Martin, J.H., Fitzwater, S.E., Gordon, R.M., Hunter, C.N., Tanner, S.J., 1993. Iron, primary production, and carbon-nitrogen flux studies during the JGOFS North Atlantic Bloom Experiment. Deep-Sea Research 40, 115–134.

Millero, F.J., Yao, W., Aicher, J., 1995. The speciation of Fe(II) and Fe(III) in natural waters. Marine Chemistry 50, 21–39.

Nelson, D.M., Treguer, P., 1992. Role of silicon as a limiting nutrient to Antarctic diatoms: evidence for kinetic studies in the Ross Sea ice edge zone. Marine Ecology Progress Series 62, 283–292.

Nolting, R.F., de Baar, H.J.W., van Bennekom, A.J., Masson, A., 1991. Cadmium, copper and iron in the Scotia Sea, Weddell Sea and Weddell/Scotia Confluence (Antarctica). Marine Chemistry 35, 219–243.

Nolting, R.F., Gerringa, L., Swagerman, R., Timmermans, K.R., de Baar, H.J.W., 1998. Fe(III) speciation in the high nutrient low chlorophyll Pacific region of the Southern Ocean. Marine Chemistry 62, 335–352, in press.

Obata, H., Karatani, H., Nakayama, E., 1993. Automated determination of iron in seawater by chelating resin concentration and chemiluminescence detection. Anal. Chem. 65, 1524–1528.

Orsi, A.H., Whithworth, T., Nowlin, W.D. Jr., 1995. On the meridional extent and fronts of the Antarctic Circumpolar Current. Deep-Sea Research 42, 641–673.

Powell, R.T., Whitney King, D., Landing, W.M., 1995. Iron distributions in surface waters of the south Atlantic. Marine Chemistry 50, 13–20.

Quéguiner, B., Tréguer, P., Peeken, I., Scharek, R., 1997. Biogeochemical dynamics and the silicon cycle in the Atlantic sector of the Southern Ocean during austral spring 1992. Deep-Sea Research II 44, 69–91.

Read, J.F., Pollard, R.T., Morrison, A.I., Symon, C., 1995. On the southerly extent of the Antarctic Circumpolar Current in the southeast Pacific. Deep-Sea Research II 42, 933–954.

Robertson, J.E., Watson, A.J., 1995. A summer-time sink for atmospheric carbon dioxide in the Southern Ocean between 88°W and 80°E. Deep-Sea Research II 42, 1081–1091.

Rue, E.L., Bruland, K.W., 1995. Complexation of iron (III) by natural organic ligands in the Central North Pacific as determined by a new competitive ligand equilibration/adsorptive cathodic stripping voltammetric method. Marine Chemistry 50, 117–138.

Russell, M.J., Daniel, R.M., Hall, A.J., 1993. On the emergence of life via catalytic iron-sulphide membranes. Terra Nova 5, 343–347.

Rutgers van der Loeff, M.M., Moore, W.S., Determination of natural radioactive tracers. In: Grasshoff, K., Ehrhardt, M., Kremling, K. (Eds.), Methods of Seawater Analysis, 3rd edn., Verlag Chemie, Weinheim, in press.

Rutgers van der Loeff, M., Friedrich, J., Bathmann, U.V., 1997. Carbon export during the spring bloom at the Antarctic Polar Front determined with the natural tracer 234Th. Deep-Sea Research II 44, 457–478.

Saager, P.M., de Baar, H.J.W., Burkill, P.H., 1989. Manganese and iron in Indian Ocean waters. Geochim. Cosmochim. Acta 53, 2259–2267.

Sarthou, G., Jeandel, C., Brisset, L., Amouroux, D., Besson, T., Donard, O.F.X., 1997. Fe and H_2O_2 distributions in the upper water column in the Indian sector of the Southern Ocean. Earth Planet. Sci. Lett. 147, 83–92.

Savidge, G., Harbour, D., Gilpin, L.C., Boyd, P.W., 1995. Phytoplankton distributions and production in the Bellingshausen Sea, Austral spring 1992. Deep-Sea Research II 42, 1201–1224.

Scharek, R., van Leeuwe, M.A., de Baar, H.J.W., 1997. Responses of Antarctic phytoplankton to the addition of trace metals. Deep-Sea Research II 44, 209–228.

Sedwick, P.N., Edwards, P.R., Mackey, D.J., Griffiths, F.B., Parslow, J.S., 1997. Iron and manganese in surface waters of the Australian subantarctic region. Deep-Sea Research 44 (7), 1239–1253.

Sildam, J., 1995. Cruise ANTARKTIS XII/4 of RV 'Polarstern' in 1995: CTD-Report. Berichte zur Polarforschung, 178, 64 pp.

Smetacek, V., de Baar, H.J.W., Bathmann, U.V., Lochte, K., Rutgers van der Loeff, M.M., 1997. Ecology and biogeochemistry of the Antarctic Circumpolar Current during Austral Spring: a summary of Southern Ocean JGOFS cruise ANT X/6 of RV polarstern. Deep-Sea Research II 44, 1–22.

Smith, W.O. Jr., Nelson, D.M., DiTullio, G.R., Leventer, A.R., 1996. Temporal and spatial patterns in the Ross Sea: phytoplankton biomass, elemental composition, productivity and growth rates. J. Geophys. Res. 101 (C8), 18455–18465.

Sommer, U., 1986. Nitrate- and silicate-competition among Antarctic phytoplankton. Marine Biology 91, 345–351.

Stoll, M.H.C., van Aken, H.M., de Baar, H.J.W., Kraak, M., 1996a. Carbon dioxide characteristics of water masses in the northern North Atlantic Ocean. Marine Chemistry 55, 217–232.

Stoll, M.H.C., van Aken, H.M., de Baar, H.J.W., de Boer, C.J., 1996b. Meridional carbon dioxide transport in the northern North Atlantic Ocean. Marine Chemistry 55, 205–216.

Sullivan, C.W., Arrigo, K.R., McClain, C.R., Comiso, J.C., Firestone, J., 1993. Distribution of phytoplankton blooms in the Southern Ocean. Science 262, 1832–1837.

Takeda, S., Kamatani, A., Kawanobe, K., 1995. Effects of nitrogen and iron enrichments on phytoplankton communities in the northwestern Indian Ocean. Marine Chemistry 50, 229–241.

Taylor, S.R., 1964. Abundance of chemical elements in the continental crust: a new table. Geochim. Cosmochim. Acta 28, 1273–1285.

Timmermans, K.R., Swagerman, M., Nolting, R.F., van Leeuwe, M.A., Gerringa, L., de Jong, J.T.F., de Baar, H.J.W., 1997.

Availability of iron in HNLC waters of the Southern Pacific Ocean. Abstract GEOC 120, 213th American Chemical Society National Meeting, San Francisco.

Timmermans, K.R., van Leeuwe, M.A., de Jong, J.T.M., McKay, R., Nolting, R.F., Witte, H., van Ooyen, J., Swagerman, M., Kloosterhuis, H., de Baar, H.J.W., 1998. On iron limitation in the Southern Pacific and Antarctic Oceans. Marine Ecology Progress Series 166, 27–41.

Trenberth, K.E., Large, W.G., Olson, J.G., 1990. The mean annual cycle in global ocean wind stress. Journal of Physical Oceanography 20, 1742–1760.

Turner, D., Owens, N., Priddle, J. (Eds.), 1995. Southern Ocean JGOFS: The U.K. 'STERNA' Study in the Bellingshausen Sea. Deep-Sea Research II, 42, 905–1335.

van Leeuwe, M.A., 1997. A Barren Ocean: Iron and Light Interactions with Phytoplankton Growth in the Southern Ocean. PhD Thesis, Univ. of Groningen, ISBN 903670785 4, 189 pp.

van Leeuwe, M.A., Scharek, R., de Baar, H.J.W., de Jong, J.T.M., Goeyens, L., 1997. Iron enrichment experiments in the Southern Ocean: physiological responses of a plankton community. Deep-Sea Research II 44, 189–208.

van Leeuwe, M.A., de Baar, H.J.W., Veldhuis, M.J.W., 1998a. Pigment distribution in the Pacific region of the Southern Ocean (autumn 1995). Polar Biology 19, 348–353.

van Leeuwe, M.A., Timmermans, K.R., Witte, H.J., Kraay, G.W., de Baar, H.J.W., 1998b. Effects of iron limitation on chromatic adaptation by natural phytoplankton communities in the Southern Ocean. Marine Ecology Progress Series 166, 43–52.

Veth, C., Peeken, I., Scharek, R., 1997. Physical anatomy of fronts and surface waters in the ACC near the 6 degree West meridian during austral spring 1992. Deep-Sea Research II 44, 23–50.

Wächtershäuser, G., 1992. Groundworks for an evolutionary biochemistry; the iron-sulphur world. Progress in Biophysics and Molecular Biology 58, 85–201.

Waite, T.D., Szymczak, R., Esprey, Q.I., Furnas, J.M., 1995. Diel variations in iron speciation in northern Australian shelf waters. Marine Chemistry 50, 79–92.

Westerlund, S., Öhman, P., 1991. Iron in the water column of the Weddell Sea. Marine Chemistry 35, 199–217.

Whitworth, T. III, 1988. The Antarctic Circumpolar Current. Oceanus 31, 53–58.

Wu, J., Luther, G.W. III, 1994. Size-fractionated iron concentrations in the water column of the Northwest Atlantic Ocean. Limnology and Oceanography 39, 1119–1129.